

**Robust Estimation of Coupling Loss Factors  
From Finite Element Analysis**

**A.N. Thite and B.R. Mace**

ISVR Technical Memorandum No 935

May 2004



## SCIENTIFIC PUBLICATIONS BY THE ISVR

*Technical Reports* are published to promote timely dissemination of research results by ISVR personnel. This medium permits more detailed presentation than is usually acceptable for scientific journals. Responsibility for both the content and any opinions expressed rests entirely with the author(s).

*Technical Memoranda* are produced to enable the early or preliminary release of information by ISVR personnel where such release is deemed to be appropriate. Information contained in these memoranda may be incomplete, or form part of a continuing programme; this should be borne in mind when using or quoting from these documents.

*Contract Reports* are produced to record the results of scientific work carried out for sponsors, under contract. The ISVR treats these reports as confidential to sponsors and does not make them available for general circulation. Individual sponsors may, however, authorize subsequent release of the material.

### COPYRIGHT NOTICE

(c) ISVR University of Southampton All rights reserved.

ISVR authorises you to view and download the Materials at this Web site ("Site") only for your personal, non-commercial use. This authorization is not a transfer of title in the Materials and copies of the Materials and is subject to the following restrictions: 1) you must retain, on all copies of the Materials downloaded, all copyright and other proprietary notices contained in the Materials; 2) you may not modify the Materials in any way or reproduce or publicly display, perform, or distribute or otherwise use them for any public or commercial purpose; and 3) you must not transfer the Materials to any other person unless you give them notice of, and they agree to accept, the obligations arising under these terms and conditions of use. You agree to abide by all additional restrictions displayed on the Site as it may be updated from time to time. This Site, including all Materials, is protected by worldwide copyright laws and treaty provisions. You agree to comply with all copyright laws worldwide in your use of this Site and to prevent any unauthorised copying of the Materials.

UNIVERSITY OF SOUTHAMPTON  
INSTITUTE OF SOUND AND VIBRATION RESEARCH  
DYNAMICS GROUP

**Robust Estimation of Coupling Loss Factors  
from Finite Element Analysis**

by

**A.N. Thite and B.R. Mace**

ISVR Technical Memorandum No: 935

May 2004

Authorised for issue by  
Professor M.J. Brennan  
Group Chairman

© Institute of Sound & Vibration Research



## Abstract

There are well-established techniques by which the coupling loss factors (CLFs) of statistical energy analysis (SEA) can be estimated from finite element analysis (FEA). These typically give estimates based on FEA of a single, selected system. A slightly different choice of system would give different estimates. There is therefore a need for robust methods that give good estimates of the SEA average CLFs, independent of the details of the chosen system. Furthermore, estimates of variance, confidence limits, etc. of estimated CLFs are also of interest. This work discusses approaches to this problem. Two approaches are suggested. These involve attempts to randomise the properties of the system being analysed. The first involves component modal descriptions of the individual subsystems. Perturbations of the subsystem modal properties can then be related to perturbations in the modes of the assembled structure and hence to the energies and CLFs. The second approach assumes that the statistics of the modal properties (natural frequencies and modes shapes) of the system analysed by FEA are a fair representation, when taken over a wide enough frequency range, of the statistics of the modes of the SEA ensemble. The modes of the system are randomly sampled to provide robust estimates of CLFs, together with estimates of variance, confidence limits etc. Qualitative assessment of dependence of variations on the number of modes in the frequency band of analysis and the modal overlap are discussed. A hypothesis concerning the dependence of the variance on the number of modes and the modal overlap is proposed. Numerical examples are presented. The methods are developed and applied as post-processors to the output of a conventional FE package.



## Contents

<b>Abstract</b>	
<b>1. Introduction</b>	1
1.1. SEA formulation	3
1.2. Energy flow model and SEA	4
<b>2. Influence of various terms on variability of EIC</b>	5
2.1. Coupling loss factor in terms of EIC	7
2.1.1. Low modal overlap considerations	7
2.1.2. Moderate modal overlap considerations	8
2.2. Ensemble average estimates and variance of EIC	9
2.3. Variance of coupling loss factor	12
2.3.1. Variance at low modal overlap	12
2.3.2. Variance at moderate modal overlap	15
<b>3. Perturbation approach to variability estimates</b>	17
3.1. Perturbation relation between local and global modal properties	17
<b>4. Random sampling of modes</b>	18
<b>5. Numerical example: baseline structure and results for very wide frequency bandwidths</b>	19
5.1. Moderate modal overlap approximations for ACLF	26
5.2. ACLF statistics from the perturbational approach: numerical results	26
5.2.1. Effect of number of modes in band on variability	30
5.3. CLF statistics from random sampling	32
<b>6. Approximations with low mode count</b>	34
6.1. Mode spacing	31
6.2. Hypothesis	36
<b>7. Numerical results for various shapes</b>	38
<b>8. Discussion and conclusions</b>	40
<b>9. References</b>	43



## 1. Introduction

Energy based modelling approaches are often used to describe high frequency vibrational behaviour of complex structures in some average or approximate way. The structure is divided into substructures and the response is described in terms of the total time average substructure energies  $E$  and input powers  $P_{in}$ . The most important of energy methods is statistical energy analysis (SEA) [1]. It is used in modelling of physical systems which share gross characteristics but differ in detailed properties. These differences in detail may have significant influence on the high frequency vibrational behaviour of the system. Since these effects are unpredictable for every realisation of the system, probabilistic vibrational models of SEA type might be used. In SEA, the time and ensemble average coupling power between two subsystems is assumed to be proportional to the difference in time and ensemble averaged modal energies of components. The constants of proportionality are related to the coupling loss factors. The chief advantages of SEA are: a) complex systems are represented in terms of a small number of gross parameters, allowing easy interpretation of results and sensitivity analysis and b) although the terms involved are gross in nature they are easily related to physical characteristics. The estimates of coupling loss factors are usually made on the basis of an idealised model of the system under investigation. Thus SEA involves many approximations and assumptions, the validity of which are not known *a priori*. Recently, SEA-like methods that do not require all the assumptions of classical SEA to be valid were discussed by Mace [2] using an energy distribution model. That mainly concerned provision for indirect coupling loss factors, as defined elsewhere [3].

SEA may be used for either theoretical predictions or experimental design and analysis. In theoretical predictions, the system concerned is highly idealised with simplifying assumptions about the coupling between subsystems often being made. Generally, estimations are based on an asymptotic wave approach which results in coupling loss factors that are independent of damping loss factors. However, damping dependence of CLF in the low modal overlap regions was shown in Ref [4]. Analytical expressions based on the wave approach for a special case of rectangular plates with coupling allowing only flexural motion was developed for coupling loss factors in Ref [5]. This formulation also indicated the damping dependence of CLFs in the low modal overlap region. It is extremely difficult to obtain these analytical expressions for complicated geometries. In the asymptotic high modal overlap approach, however, any shape is similarly treated, with only area and perimeter being important. It is

still an issue to obtain coupling loss factors for the frequencies where the modal overlap is smaller than unity and coupling is strong. Experimental SEA could be used in these cases: the power injection method can be used to obtain coupling loss factors. In cases like these, complicated geometry or complicated coupling, FE analysis can be very useful to estimate CLFs numerically. In previous approaches an FE model of two subsystems is produced, and estimates of subsystem energy and input power found. In the most general approach ([6] and later, in this report) true energy and input power for ‘rain-on-the-roof’ excitation are found, while in other approaches discretely sampling of power and energy for point excitation and point response are used. Ref [6] contains references to such approaches, which include [7]. The coupling loss factor so estimated from a one-off analysis is referred to as the *apparent coupling loss factor* (ACLF) [7] to distinguish it from ensemble based estimates.

In Ref [8] numerical studies were carried out to assess the variations at low modal overlap for one and two-dimensional systems. Large variations were seen in the estimates of coupling loss factors when the modal overlap was smaller than unity. In this study at least 14 modes existed within the frequency band considered. Also only ten power injection points were used, which might result in preferential excitation of certain modes. This might, however, be taken as a particular physical test set-up. In that study only regular shape structures were used in the analysis. Recently [9], numerical studies were used to conclude that the apparent coupling loss factors are somewhat log-normal in distribution. Here, again, regular shape structures were used. The excitation was assumed to be ‘rain’. A limited sample size of 30 is used to estimate ensemble average quantities. Since the analysis is based on 1/3 octave conversion, it is very difficult to conclude the exact influence of the number of modes and the modal overlap on the variability in estimated coupling loss factors. Also it is suggested that the matrix becomes ill-conditioned because of the presence of errors in the measured energy values, which is debatable: the ill-conditioning is possibly inherent in the model at low modal overlap and for few modes in band.

In this report, the variability of the apparent coupling loss factor at low modal overlap and in the presence of small number of modes is addressed. The theoretical basis for understanding the variability at low and high modal overlap is discussed. Initially, only systems containing two subsystems are considered. Mode participation factor statistics suggested in [10] are principal in these discussions. Some interesting influences of mode spacing on coupling loss factor variability are also discussed. Two methods to reduce this variability and produce

robust estimates of CLFs are suggested. First, a perturbation approach, the local modal perturbation (LMP) method [11], is used in obtaining global mode statistics. Using energy influence coefficients, apparent coupling loss factors are obtained. The ensemble is formed using global mode statistics. Secondly, an approach based on random mode sampling is introduced. The results from both approaches are compared and relative benefits are discussed. Based on several numerical simulations and the theoretical background, a hypothesis is presented for dependence of variability on modal overlap and number of modes in the frequency bandwidth.

In the rest of Section 1 a review is given of the basic formulation to estimate coupling loss factors from an energy distribution model for a system consisting of two subsystems. Section 2 covers discussion on the influence of various terms in the energy influence coefficients on the variability. A discussion on ensemble estimates in terms of the mode participation factors is presented. Following this a brief review is given of a perturbation approach that is used to obtain global mode statistics. An alternative approach of random mode selection is discussed in Section 4. Results of numerical study and suggested hypothesis are described in next two sections.

### 1.1. SEA formulation

The SEA equations in terms of damping and coupling loss factors, and total energies of subsystems can be written as

$$\mathbf{P}_m = \mathbf{L}\mathbf{E} \quad (1)$$

where  $\mathbf{P}_m$  and  $\mathbf{E}$  are ensemble averages of input power and subsystem energies,  $\mathbf{L}$  is a matrix of damping and coupling loss factors and is given by

$$\mathbf{L} = \omega \text{diag}(\eta_j) + \omega \begin{bmatrix} \eta_{12} + \eta_{13} + \dots & -\eta_{21} & \dots \\ -\eta_{12} & \eta_{21} + \eta_{23} + \dots & \dots \\ \vdots & \vdots & \ddots \end{bmatrix} \quad (2)$$

Here  $\eta_j$  and  $\eta_{ij}$  are damping and coupling loss factors respectively. To maintain energy conservation, the columns of the matrix of coupling loss factors sum to zero. The elements of  $\mathbf{L}$  must also satisfy the consistency relation,

$$n_i \eta_{ij} = n_j \eta_{ji} \quad (3)$$

where  $n_i$  is the asymptotic modal density of subsystem  $i$ .

SEA theory involves number of assumptions and approximations. If these are valid then the SEA equations are valid in an ensemble average sense, i.e. when powers and energies are averaged over an ensemble of similar, but slightly different systems. However, when applied to an individual system, they are assumed to be good approximations only when averaged over a suitably wide frequency range. In classical SEA, if two subsystems are not physically connected, the associated coupling loss factors should be zero i.e. indirect coupling loss factors are zero. Also it is assumed that the coupling loss factors are positive and independent of damping loss factors. The modal energies above correspond to subsystem energies in isolation or actual energies when coupled.

## 1.2. Energy distribution model and SEA

The energy distribution (ED) model can also be used in obtaining parameters similar to those of SEA [2]. If an ED model is formed, following [2], then

$$\begin{aligned} \mathbf{E} &= \mathbf{A} \mathbf{P}_{in} \\ \mathbf{P}_{in} &= \mathbf{X} \mathbf{E}, \quad \mathbf{X} = \mathbf{A}^{-1} \end{aligned} \quad (4)$$

where  $\mathbf{A}$  is a matrix of energy influence coefficients. In this study, as in Ref [2], the elements of this matrix are found from the modal properties of the system. The only major simplifying assumptions required here are linearity and ‘rain’ excitation. The inverse  $\mathbf{X}$  of  $\mathbf{A}$ , however, need not be in the special form of the SEA matrix  $\mathbf{L}$  in equation (1). In particular, since it is usually a ‘one-off’ estimate, it is strictly a matrix of ACLFs. Furthermore, there may be non-zero indirect CLFs.

It is assumed that both the time average kinetic energy and time average potential energy are equal. For the system with two subsystems, the energy influence coefficient  $A_{12}$  (EIC), which relates energy in subsystem 1 with excitation in subsystem 2, is given by [2]

$$A_{12} = \frac{E_2^{(1)}}{P_{in2}} = \frac{2T_2^{(1)}}{P_{in2}} = \frac{\sum_j \sum_k \Gamma_{jk} \psi_{jk}^{(1)} \psi_{jk}^{(2)}}{\sum_j \Delta_j \Gamma_{jj} \psi_{jj}^{(2)}} \quad (5)$$

where the subscripts  $j$  and  $k$  refer to the  $j^{\text{th}}$  and  $k^{\text{th}}$  modes of the system, where  $T_2^{(1)}$  is the total kinetic energy in subsystem 1, and is given by

$$T_2^{(1)} = 2S_f \sum_j \sum_k \Gamma_{jk} \psi_{jk}^{(2)} \psi_{jk}^{(1)} \quad (6)$$

$P_{in2}$  is the power input into subsystem 2, and is given by

$$P_{in2} = 2S_f \sum_j 2\Delta_j \Gamma_{jj} \psi_{jj}^{(2)} \quad (7)$$

while  $\Gamma_{jk}$  is cross modal power given by

$$\Gamma_{jk}(\omega) = \frac{1}{\Omega} \int_{\omega \in \Omega} \frac{1}{4} \omega^2 \beta_{jk}(\omega) d\omega \quad (8)$$

and  $\psi_{jk}^{(1)}$  is cross-mode participation factor given by

$$\psi_{jk}^{(1)} = \int_{x \in I} \rho(x) \phi_j(x) \phi_k(x) dx \quad (9)$$

The modal receptance  $\alpha(\omega) = \frac{1}{\omega_j^2 - \omega^2 + i\Delta_j \omega}$  and for viscous damping  $\Delta_j = 2\zeta_j \omega_j = \eta_j \omega_j$

and  $\beta_{jk}(\omega) = \text{Re}\{\alpha_j(\omega)\alpha_k(\omega)^*\}$ . Note that for a system made of two subsystems the following relations hold good:  $\psi_{jj}^{(1)} + \psi_{jj}^{(2)} = 1$ ,  $\psi_{jk}^{(1)} + \psi_{jk}^{(2)} = 0$  and  $\sigma_{\psi}^{(1)2} = \sigma_{\psi}^{(2)2}$ . These relations will be utilised later in simplifying various terms.

The cross-modal power  $\Gamma_{jk}(\omega)$  is independent of spatial variations and depends on natural frequencies and bandwidths of modes only. Also it is a global parameter, i.e. it is the same for all subsystems, whereas the cross-mode participation factors  $\psi_{jk}$  depend on the local modal behaviour of the system within each subsystem. The cross modal participation factors do not change with frequency and are only spatially dependent. The ‘self’ terms in cross-modal participation factors i.e. the mode participation factors, indicate the energy contained in each subsystem for a mode. The cross terms are largest.

## 2. Influence of various terms on variability of EIC

In order to gain insight into variability and robust estimation of coupling loss factor, the effects of the different terms in the EIC are discussed in this section. In [10], a detailed

analysis of this effect on CLFs and indirect CLFs was carried out. From the point of view of variability of ACLFs, certain points are repeated in this report.

Assuming that the damping bandwidth is the same for all modes, (of course this is another source of variability) equation (5) simplifies to

$$A_{12} = \frac{1}{\omega\eta} \frac{\sum_j \sum_k \Gamma_{jk} \psi_{jk}^{(1)} \psi_{jk}^{(2)}}{\sum_j \Gamma_{jj} \psi_{jj}^{(2)}} \quad (12)$$

In terms of the self and cross terms in modal power and modal participation factor, the above equation can be rewritten as

$$\begin{aligned} A_{12} &= \frac{1}{\omega\eta} \frac{\sum_j \Gamma_{jj} \psi_{jj}^{(1)} \psi_{jj}^{(2)} + \sum_j \sum_{k \neq j} \Gamma_{jk} \psi_{jk}^{(1)} \psi_{jk}^{(2)}}{\sum_j \Gamma_{jj} \psi_{jj}^{(2)}} \\ &= A_{12(1)} + A_{12(2)} \end{aligned} \quad (13)$$

The self terms in the cross-mode power [10] for large frequency bandwidths  $\Omega$  of excitation can be simplified as

$$\Gamma_{jj} \approx \frac{\pi}{8\Omega\omega\eta} = \frac{\pi}{8\Omega\Delta} \quad (14)$$

so long as the natural frequency  $\omega_j$  lies in the excitation band, otherwise  $\Gamma_{jj} = 0$ . It was shown in [10] that

$$\begin{aligned} \Gamma_{jk} &\approx \frac{M_{jk}^2}{1 + M_{jk}^2} \frac{\pi}{8\Omega\Delta} \\ &= \mu_{jk} \frac{\pi}{8\Omega\Delta} \end{aligned} \quad (15)$$

where  $M_{jk}$  is modal overlap of two modes, and is defined as the ratio of the damping bandwidth to the modal spacing. With these simplifications (12) reduces to

$$A_{12} \cong \frac{1}{\omega\eta} \frac{\sum_j \psi_{jj}^{(1)} \psi_{jj}^{(2)} + \sum_j \sum_{k \neq j} \mu_{jk} \psi_{jk}^{(1)} \psi_{jk}^{(2)}}{\sum_j \psi_{jj}^{(2)}} \quad (16)$$

which contains terms from mode participation factors  $\psi$  and  $\mu_{jk}$ . The modal power terms  $\Gamma_{jj}$  are seen to disappear from the expression. Broadly the assumption behind this are valid if

the modal bandwidth is small compared to the excitation bandwidth so that a mode either lies inside or outside the excitation band. The statistics of the mode participation factors  $\psi_{jk}$ , together with those of the modal overlap  $\mu_{jk}$  of two modes, are however expected to influence the variability in energy influence coefficients to a possibly large extent, and hence influence the variability in the ACLFs which are found by inverting the EIC matrix.

## 2.1. Coupling loss factor in terms of EIC

For a system comprising of two subsystems the inverse of energy influence coefficient matrix can be written as

$$\mathbf{A}^{-1} = \mathbf{X} = \omega\eta \begin{bmatrix} \frac{A_{22}^p}{A_{11}^p A_{22}^p - A_{12}^p A_{21}^p} & -\frac{A_{12}^p}{A_{11}^p A_{22}^p - A_{12}^p A_{21}^p} \\ -\frac{A_{21}^p}{A_{11}^p A_{22}^p - A_{12}^p A_{21}^p} & \frac{A_{22}^p}{A_{11}^p A_{22}^p - A_{12}^p A_{21}^p} \end{bmatrix} \quad (17)$$

where, for example,  $A_{11}^p = \omega\eta A_{11}$  is the dissipated power in subsystem 1 per unit input power into subsystem 1. An estimate of the coupling loss factor  $\eta_{12}$  is then obtained from the relation

$$\hat{\eta}_{12} = \eta \left( \frac{A_{22}^p}{A_{11}^p A_{22}^p - A_{12}^p A_{21}^p} - 1 \right) \quad (18a)$$

or

$$\hat{\eta}_{12} = \eta \frac{A_{21}^p}{A_{11}^p A_{22}^p - A_{12}^p A_{21}^p} \quad (18b)$$

Since the coupling loss factor is based on frequency average quantities rather than ensemble averages, it is referred here as the apparent coupling loss factor (ACLF) and indicated by superscript  $\hat{\bullet}$ .

### 2.1.1. Low modal overlap considerations

For low modal overlap  $M_{jk}$  for  $j \neq k$  will be negligible. The energy influence coefficient in equation (12) is thus dependent only on mode participation factors. Therefore,

$$A_{11} \approx \frac{1}{\omega\eta} \frac{\sum_j \psi_{jj}^{(1)} \psi_{jj}^{(1)}}{\sum_j \psi_{jj}^{(0)}} \quad (19a)$$

Using statistics of mode participation factors within the frequency bandwidth, when this bandwidth is large so that many modes lie within it,

$$A_{11} \equiv \frac{1}{\omega\eta} \frac{v_1^2 + \sigma_\psi^2}{v_1} \quad (19b)$$

where  $v_1$  is the mean and  $\sigma_\psi^2 = \mathbb{E}[(\psi_{jj}^{(1)} - v_1)^2]$  is the variance of mode participation factors of subsystem 1 within the excitation band. For a large frequency band they tend to ensemble average values. The mean of the participation factors tends to the fractional modal density under such situations (i.e.  $\frac{n_1}{n_1 + n_2}$ ). Since the mean and variance of the mode participation factor for the modes within the band are estimates based on a limited sample size (i.e. the actual number of modes) they will vary from the broadband ensemble based estimates.

### 2.1.2. Moderate modal overlap considerations

For higher modal overlap the cross terms in mode participation factors can contribute significantly to energy influence coefficients (equation (16)). This equation, however, can be simplified if in evaluating  $M_{jk}$  the mean mode spacing is used rather than the actual spacing.

With this assumption, the modal overlap of two modes is  $M_{jk} = \frac{M}{|j-k|}$ . This also means that

for moderate modal overlap, due to value of  $\mu_{jk}$ , consideration of interaction with only immediate neighbouring modes would be sufficient. This implies that  $\Gamma_{jk}$  is negligible if  $|k-j| > 1$ . Therefore, for these values of modal overlap

$$A_{12} \approx \frac{1}{\omega\eta} \frac{\sum_j \psi_{jj}^{(2)} \psi_{jj}^{(1)} + \sum_j \mu_{jj+1} \psi_{jj+1}^{(2)} \psi_{jj+1}^{(1)} + \sum_j \mu_{j-1j} \psi_{j-1j}^{(2)} \psi_{j-1j}^{(1)}}{\sum_j \psi_{jj}^{(2)}} \quad (20)$$

since  $\mu_{jj+1} = \mu_{j-1j}$  and  $\psi_{jj+1}$  and  $\psi_{j-1j}$  have zero mean and the same standard deviations, the expression for  $A_{11}$  reduces to

$$A_{11} \equiv \frac{1}{\omega\eta} \frac{v_1^2 + \sigma_\psi^2 + 2 \frac{M^2}{1+M^2} \sigma_{\psi_1}^2}{v_1} \quad (21)$$

where  $\sigma_{\psi_1}$  is the standard deviation of the cross participation factors  $\psi_{j,j+1}$ , i.e. the cross participation factors for neighbouring modes.

## 2.2. Ensemble average estimates and variance of EIC

In energy formulations, the subsystem energies for a specific system under specific excitation over a specific frequency band may differ from ensemble average SEA predictions [1,2,5,8-9 and 12]. These SEA expressions are based on various approximations and assumptions. Of course it may also be that the SEA approximate assumptions are not valid - for example there may be strong coupling so that classical expressions do not give the right average. Some of the reasons for variability in SEA predictions are [2];

- a. The excitation may be frequency dependent, or may it not have spatial dependence assumed for the 'rain' excitation. For example, various modes may be excited preferentially.
- b. Different modes may have different loss factors, so some may respond preferentially.
- c. The damping may be large enough or the bandwidth narrow enough, such that non-resonant modes contribute substantially.

These are all minor causes of variability. A more fundamental cause of variability in the responses of individual systems arises from finite frequency band excitation and the statistics of those modes which happen to lie in the band. The subsystem energies depend on cross modal participation factors, while the input power depends on self terms only, and hence the energy influence coefficients are dependent on both self and cross modal participation factors.

As discussed earlier, EIC estimates are based on frequency averages. For the classical SEA formulation, however, ensemble average quantities are necessary. It is of interest to consider ensemble averages in addition to frequency averages.

The ensemble average estimate of one of the power ratios

$$E[A_{11}^p] = E[V_1] + E\left[\frac{\sigma_\psi^2}{V_1}\right] \quad (22)$$

Since the fractional modal density is dependent only on subsystem dynamics, while the standard deviation is dependent on the connection between subsystems, they are assumed independent of each other. Therefore the frequency and ensemble average power ratio is given by

$$E[A_{11}^p] = E[v_1] + \frac{E[\sigma_\psi^2]}{E[v_1]} \quad (23a)$$

or

$$\bar{A}_{11}^p = \bar{v}_1 + \frac{\bar{\sigma}_\psi^2}{\bar{v}_1} \quad (23b)$$

where  $\bar{\bullet}$  denotes the expectation or ensemble average.

It is assumed above that the standard deviation used is unbiased. The variation of the frequency average from the above can be quantified by the variance of the energy influence coefficient, which can be written as,

$$\text{var}[A_{11}] = \frac{1}{\Delta^2} E\left[(A_{11}^p - \bar{A}_{11}^p)^2\right] \quad (25)$$

It is assumed here that the damping parameter can be estimated with certainty. After expansion the variance is given by

$$\begin{aligned} \text{var}[A_{11}] &= \frac{1}{\Delta^2} \left\{ E\left[\left(\frac{v_1^2 + \sigma_\psi^2}{v_1}\right)^2\right] + E\left[\left(\frac{\bar{v}_1^2 + \bar{\sigma}_\psi^2}{\bar{v}_1}\right)^2\right] - 2E\left[\left(\frac{v_1^2 + \sigma_\psi^2}{v_1}\right)\left(\frac{\bar{v}_1^2 + \bar{\sigma}_\psi^2}{\bar{v}_1}\right)\right] \right\} \\ &= \frac{1}{\Delta^2} \left\{ E\left[\left(v_1 + \frac{\sigma_\psi^2}{v_1}\right)^2\right] - E\left[\left(\frac{\bar{v}_1^2 + \bar{\sigma}_\psi^2}{\bar{v}_1}\right)^2\right] \right\} \\ &= \frac{1}{\Delta^2} \left\{ E\left[v_1^2 + \frac{\sigma_\psi^4}{v_1^2} + 2\sigma_\psi^2\right] - \bar{v}_1^2 - \frac{\bar{\sigma}_\psi^4}{\bar{v}_1^2} - 2\bar{\sigma}_\psi^2 \right\} \end{aligned}$$

For an unbiased estimate  $E[\sigma_\psi^2] = \bar{\sigma}_\psi^2$ , therefore

$$\begin{aligned} &= \frac{1}{\Delta^2} \left\{ E[v_1^2] + \frac{E[\sigma_\psi^4]}{E[v_1^2]} + 2\bar{\sigma}_\psi^2 - \bar{v}_1^2 - \frac{\bar{\sigma}_\psi^4}{\bar{v}_1^2} - 2\bar{\sigma}_\psi^2 \right\} \\ &= \frac{1}{\Delta^2} \left\{ E[v_1^2] + \frac{E[\sigma_\psi^4]}{E[v_1^2]} - \bar{v}_1^2 - \frac{\bar{\sigma}_\psi^4}{\bar{v}_1^2} \right\} \end{aligned}$$

Standard statistical expressions are available for the above expectations based on sample size. In this case the sample size is taken as the expected number of modes in the frequency band. If standard expression were to be used the assumption that the particular bandwidth would contain a fixed number of modes must be made. If bandwidth considered is small, this will not be true and the number of modes in the band will vary significantly. However, if the bandwidth is larger the number of modes contained  $N \approx \bar{N}$  i.e. approximately the average

number of modes, where  $\bar{\bullet}$  indicates the ensemble average of the parameter. In the derivations that follow, it is assumed that a large number of modes exist in the bandwidth so that the error due to the above assumption is very small. Therefore using standard statistical expressions [12],

$$\begin{aligned}\text{var}[A_{11}] &= \frac{1}{\Delta^2} \left\{ \bar{v}_1^2 + \frac{\bar{\sigma}_\psi^2}{N} + \frac{\bar{\sigma}_\psi^4 + \frac{\bar{\sigma}_\psi^4}{N}}{\bar{v}_1^2 + \frac{\bar{\sigma}_\psi^2}{N}} - \bar{v}_1^2 - \frac{\bar{\sigma}_\psi^4}{\bar{v}_1^2} \right\} \\ &= \frac{1}{\Delta^2} \left\{ \frac{\bar{\sigma}_\psi^2}{N} + \frac{\bar{\sigma}_\psi^4 + \frac{\bar{\sigma}_\psi^4}{N}}{\bar{v}_1^2 + \frac{\bar{\sigma}_\psi^2}{N}} - \frac{\bar{\sigma}_\psi^4}{\bar{v}_1^2} \right\} \\ &= \frac{1}{\Delta^2} \left\{ \frac{\bar{\sigma}_\psi^2}{N} + \frac{\bar{\sigma}_\psi^4}{\bar{v}_1^2 + \frac{\bar{\sigma}_\psi^2}{N}} + \frac{\bar{\sigma}_\psi^4}{N \left( \bar{v}_1^2 + \frac{\bar{\sigma}_\psi^2}{N} \right)} - \frac{\bar{\sigma}_\psi^4}{\bar{v}_1^2} \right\}\end{aligned}$$

For a large number of modes in the band,

$$\text{var}[A_{11}] \approx \frac{1}{\Delta^2} \left\{ \frac{\bar{\sigma}_\psi^2}{N} + \frac{\bar{\sigma}_\psi^4}{\bar{v}_1^2} + \frac{\bar{\sigma}_\psi^4}{N\bar{v}_1^2} - \frac{\bar{\sigma}_\psi^4}{\bar{v}_1^2} \right\}$$

$$\text{var}[A_{11}] \approx \frac{1}{\Delta^2} \frac{\bar{\sigma}_\psi^2}{N} \left( 1 + \frac{\bar{\sigma}_\psi^2}{\bar{v}_1^2} \right) \quad (26a)$$

$$\text{var}[A_{11}] \approx \frac{1}{\Delta^2} \text{var}[A_{11}^p] \quad (26b)$$

Using the expressions  $A_{21} = \frac{1}{\Delta} (1 - A_{11}^p)$ ,  $A_{12} = \frac{1}{\Delta} \frac{v_1}{v_2} (1 - A_{11}^p)$  and  $A_{22} = \frac{1}{\Delta} \left( 1 - \frac{v_1}{v_2} (1 - A_{11}^p) \right)$ , the

variances for other EICs can be estimated. The variance here is dependent on the number of modes in the band, in fact it is the number of modes and the corresponding mode shapes that decide the individual participation factors.

### 2.3. Variance of coupling loss factor

The uncertainty in the estimation of energy influence coefficients will propagate to coupling loss factors during the inversion of the EIC matrix. The variance associated with apparent coupling loss factors can then be approximated using a Taylor series expansion about the true value of the coupling loss factor.

Let the perturbed EIC matrix be written as

$$\mathbf{A} = \bar{\mathbf{A}} + \mathbf{A}_e \quad (27a)$$

From equation (5)

$$\mathbf{X} = \bar{\mathbf{X}} + \mathbf{X}_e = (\bar{\mathbf{A}} + \mathbf{A}_e)^{-1} \quad (27b)$$

Using a series expansion for the inverted matrix, and considering first order terms only,

$$\bar{\mathbf{X}} + \mathbf{X}_e = \bar{\mathbf{A}}^{-1} - \bar{\mathbf{A}}^{-1} \mathbf{A}_e \bar{\mathbf{A}}^{-1} \quad (27c)$$

assuming that  $\bar{\mathbf{X}} = \bar{\mathbf{A}}^{-1}$ , the propagated perturbation is given by

$$\mathbf{X}_e = \bar{\mathbf{A}}^{-1} \mathbf{A}_e \bar{\mathbf{A}}^{-1} \quad (28)$$

For example, the first element in the above matrix is given by

$$X_{e,11} = \bar{X}_{11}^2 A_{e,11} + \bar{X}_{11} \bar{X}_{12} A_{e,21} + \bar{X}_{11} \bar{X}_{21} A_{e,12} + \bar{X}_{12} \bar{X}_{21} A_{e,22} \quad (29)$$

#### 2.3.1. Variance at low modal overlap

The above equation can be simplified for low modal overlap and due the fact that perturbations in the EIC matrix must satisfy energy conservation. For energy conservation

$$\sum_i A_{e,i1} = 0 \text{ and } \sum_i A_{e,i2} = 0 \quad (30a)$$

For low modal overlap, from coupled system dynamics

$$\begin{aligned} A_{12} &= \frac{1}{\Delta} \left( 1 - \frac{\nu_2^2 + \sigma_\psi^2}{\nu_2} \right) = \frac{1}{\Delta \nu_2} (\nu_2 - \nu_2^2 + \sigma_\psi^2) \\ &= \frac{1}{\Delta \nu_2} (\nu_2 \nu_1 + \sigma_\psi^2) \end{aligned}$$

similarly

$$A_{21} = \frac{1}{\Delta \nu_1} (\nu_2 \nu_1 + \sigma_\psi^2)$$

Therefore

$$\frac{A_{12}}{A_{21}} = \frac{v_1}{v_2}$$

From this

$$A_{e,12} = \frac{v_1}{v_2} A_{e,21} \quad (30b)$$

Referring to [10], the ensemble average estimate of the inverted EIC matrix is given by

$$\bar{\mathbf{X}} = \Delta \begin{bmatrix} \frac{\bar{v}_1(\bar{v}_2^2 + \bar{\sigma}^2)}{\bar{\sigma}^2} & -\frac{\bar{v}_1(\bar{v}_1\bar{v}_2 - \bar{\sigma}^2)}{\bar{\sigma}^2} \\ -\frac{\bar{v}_2(\bar{v}_1\bar{v}_2 - \bar{\sigma}^2)}{\bar{\sigma}^2} & \frac{\bar{v}_2(\bar{v}_1^2 + \bar{\sigma}^2)}{\bar{\sigma}^2} \end{bmatrix} \quad (31)$$

This is based on the following simplification to the denominator in equation (17)

$$\begin{aligned} A_{11}^p A_{22}^p - A_{12}^p A_{21}^p &= A_{11}^p A_{22}^p - (1 - A_{11}^p)(1 - A_{22}^p) \\ &= A_{11}^p + A_{22}^p - 1 \\ &= \frac{v_1^2 + \sigma^2}{v_1} + \frac{v_2^2 + \sigma^2}{v_2} - 1 \\ &= \frac{v_2 v_1^2 + v_2 \sigma^2 + v_1 v_2^2 + v_1 \sigma^2 - v_1 v_2}{v_1 v_2} \\ &= \frac{v_1 v_2 (v_1 + v_2) + \sigma^2 (v_1 + v_2) - v_1 v_2}{v_1 v_2} \\ &= \frac{\sigma^2}{v_1 v_2} \end{aligned}$$

Since  $v_1 + v_2 = 1$ . Equation (29) therefore simplifies to

$$X_{e,11} = \frac{\Delta^2 \bar{v}_1^2 \bar{v}_2^2 A_{e,11}}{\bar{\sigma}^4} \quad (32)$$

Using the earlier ensemble definition it follows that

$$E[X_{e,11}^2] = \frac{\Delta^4 \bar{v}_1^4 \bar{v}_2^4}{\bar{\sigma}^8} E[A_{e,11}^2] \quad (33)$$

Substituting equation (26) gives

$$\begin{aligned}
E[X_{e,11}^2] &= \frac{\Delta^2 \bar{v}_1^2 \bar{v}_2^4}{N \bar{\sigma}^8} (\bar{v}_1^2 + \bar{\sigma}^2) \\
&= \frac{\Delta^2 \bar{v}_1^2 \bar{v}_2^3}{N \bar{\sigma}^6} \frac{\bar{v}_2 (\bar{v}_1^2 + \bar{\sigma}^2)}{\bar{\sigma}^2} \\
&= \frac{\Delta^2 \bar{v}_1^2 \bar{v}_2^4}{N \bar{\sigma}^6} \frac{\bar{X}_{22}}{\Delta} \\
&= \frac{\Delta^2 \bar{v}_1^2 \bar{v}_2^3}{N \bar{\sigma}^6} \frac{(\bar{\eta}_{21} + \eta)}{\eta}
\end{aligned} \tag{34}$$

Since we have assumed that the damping loss factor is known,

$$\bar{X}_{11} + \bar{X}_{e,11} = \omega \{ \eta + (\bar{\eta}_{12} + \eta_{e,12}) \}$$

and letting  $\bar{X}_{11} = \omega(\eta + \bar{\eta}_{12})$

$$\eta_{e,12} = \frac{\bar{X}_{e,11}}{\omega}$$

Therefore as earlier

$$\begin{aligned}
E[\eta_{e,12}^2] &= \frac{E[\bar{X}_{e,11}^2]}{\omega^2} \\
&= \frac{\eta \bar{v}_1^2 \bar{v}_2^3}{N \bar{\sigma}^6} (\bar{\eta}_{21} + \eta)
\end{aligned} \tag{35a}$$

and the relative variance is given by

$$\frac{\text{var}[\eta_{12}]}{\bar{\eta}_{12}} = \frac{\bar{v}_1^2 \bar{v}_2}{N \bar{\sigma}^2 (\bar{v}_1 \bar{v}_2 - \bar{\sigma}^2)^2} \left( \frac{\bar{\eta}_{21} + \eta}{\eta} \right) \tag{35b}$$

The relative variance is not only dependent on substructure properties and connection strength but also on damping loss factor. As expected, it is inversely proportional to number of modes in the bandwidth. This implies the variance is larger as the damping loss factor decreases, in accordance with observations.

### 2.3.2. Variance at moderate modal overlap

Similar estimates can be found for slightly larger values of modal overlap. As in earlier sections, the variance of the power ratio is given by

$$\begin{aligned}
\text{Var}[A_{11}^p] &= E[(A_{11}^p - \bar{A}_{11}^p)^2] \\
&= E[A_{11}^{p2}] - \bar{A}_{11}^{p2}
\end{aligned}$$

Using (21), the first term above can be expanded as

$$E[A_{11}^{p^2}] = E[v_1^2] + \frac{E[\sigma_\psi^4]}{E[v_1^2]} + 4\left(\frac{M^2}{1+M^2}\right)^2 \frac{E[\sigma_{\psi 1}^2]}{E[v_1^2]} + 2E[\sigma_\psi^2] + 4\left(\frac{M^2}{1+M^2}\right)^2 E[\sigma_{\psi 1}^2] + 4\left(\frac{M^2}{1+M^2}\right)^2 \frac{E[\sigma_\psi^2 \sigma_{\psi 1}^2]}{E[v_1^2]} \quad (37)$$

Assuming that the standard deviation estimated is unbiased and  $\sigma_\psi$  and  $\sigma_{\psi 1}$  are uncorrelated, the above expression becomes

$$E[A_{11}^{p^2}] = \bar{v}_1^2 + \frac{\bar{\sigma}_\psi^2}{N} + \frac{\bar{\sigma}_\psi^4 \left(1 + \frac{1}{N}\right) + 4\mu^2 \bar{\sigma}_{\psi 1}^4 \left(1 + \frac{1}{N}\right)}{\bar{v}_1^2 + \frac{\bar{\sigma}_\psi^2}{N}} + 2\bar{\sigma}_\psi^2 + 4\mu^2 \bar{\sigma}_{\psi 1}^2 + 4\mu^2 \frac{\bar{\sigma}_\psi^2 \bar{\sigma}_{\psi 1}^2}{\bar{v}_1^2 + \frac{\bar{\sigma}_\psi^2}{N}}$$

where the subscripts in  $\mu_{jk}$  are omitted. For larger number of modes in the frequency bandwidth this can be approximated by

$$E[A_{11}^{p^2}] = \bar{v}_1^2 + \frac{\bar{\sigma}_\psi^2}{N} + \frac{\bar{\sigma}_\psi^4 \left(1 + \frac{1}{N}\right) + 4\mu^2 \bar{\sigma}_{\psi 1}^4 \left(1 + \frac{1}{N}\right)}{\bar{v}_1^2} + 2\bar{\sigma}_\psi^2 + 4\mu^2 \bar{\sigma}_{\psi 1}^2 + 4\mu^2 \frac{\bar{\sigma}_\psi^2 \bar{\sigma}_{\psi 1}^2}{\bar{v}_1^2}$$

Therefore

$$\begin{aligned} \text{var}[A_{11}^p] &= E[A_{11}^{p^2}] - \bar{A}_{11}^{p^2} \\ &= \frac{\bar{\sigma}_\psi^2}{N} + \frac{1}{N} \left( \frac{\bar{\sigma}_\psi^4}{\bar{v}_1^2} + 4\mu^2 \frac{\bar{\sigma}_{\psi 1}^4}{\bar{v}_1^2} \right) \end{aligned} \quad (38)$$

The propagation of error to the inverted matrix can be estimated if the inverse of the EIC matrix known. The formulation can be simplified by considering

$$\sigma_e^2 = \sigma_\psi^2 + 2\mu\sigma_{\psi 1}^2 \quad (39)$$

where  $\sigma_e^2$  is referred to as the equivalent variance of the participation factors. Therefore

$$A_{11}^p = \frac{v_1^2 + \sigma_e^2}{v_1}$$

which is identical to equation (19). Hence the inverted EIC matrix can be obtained by just replacing  $\sigma_\psi$  by  $\sigma_e$  in (26). Then using (32)

$$X_{e,11} = \frac{\Delta^2 \bar{V}_1^2 \bar{V}_2^2 A_{e,11}}{\bar{\sigma}_e^4}$$

it follows that

$$\text{Var}[X_{11}] = E[X_{e,11}^2] = \frac{\Delta^4 \bar{V}_1^4 \bar{V}_2^4}{\bar{\sigma}_e^8} E[A_{e,11}^2] \quad (40)$$

Since

$$E[A_{e,11}^2] = \text{Var}[A_{11}] = \frac{1}{\Delta^2} \left\{ \frac{\bar{\sigma}_\psi^2}{N} + \frac{1}{N} \left( \frac{\bar{\sigma}_\psi^4}{\bar{V}_1^2} + 4\mu^2 \frac{\bar{\sigma}_{\psi 1}^4}{\bar{V}_1^2} \right) \right\}$$

equation (40) becomes

$$\text{Var}[X_{11}] = \frac{\Delta^2 \bar{V}_1^2 \bar{V}_2^4}{N \bar{\sigma}_e^8} \left\{ \bar{\sigma}_\psi^2 (\bar{V}_1^2 + \bar{\sigma}_\psi^2) + 4\mu^2 \bar{\sigma}_{\psi 1}^4 \right\} \quad (41)$$

Similar to (35a), the variance of the apparent coupling loss factor can be written as

$$\begin{aligned} \text{Var}[\eta_{12}] = E[\eta_{e,12}^2] &= \frac{E[\bar{X}_{e,11}^2]}{\omega^2} \\ &= \frac{\eta^2 \bar{V}_1^2 \bar{V}_2^4}{N \bar{\sigma}_e^8} \left\{ \bar{\sigma}_\psi^2 (\bar{V}_1^2 + \bar{\sigma}_\psi^2) + 4\mu^2 \bar{\sigma}_{\psi 1}^4 \right\} \end{aligned} \quad (42)$$

Here the variance is dependent on substructure properties, connection strength and damping in the structures. In general terms, it is inversely proportional to the equivalent variance of the participation factors. Since the equivalent variance is dependent on modal overlap, the variance of the apparent coupling loss factors is inversely proportional to the modal overlap. There is also a term in the numerator that contains modal overlap, but the power of that term is much smaller than that in the denominator. This also indicates that, whatever the number of modes in the frequency band, variability reduces with increasing modal overlap. It actually means that the ratio of dissipated power to input power in the excited system tends to unity i.e. very little power is left in the unexcited system to be dissipated. This is seen to be true from (42) for any number of modes or whatever the bandwidth.

### 3. The perturbation approach to variability estimates

For estimation of the EICs, a fixed interface component mode synthesis [13] approach is used. In this section a perturbation approach is used to randomise subsystem properties and hence the system properties. A brief review is given below of how randomisation of subsystems is used in obtaining global mode statistics [11].

Variability in the subsystem properties is represented in terms of variability in the subsystems modes. In general, even if CMS approach were adopted the global modal analysis would be computationally expensive. Therefore it is not feasible to repeat the FEA many times, with many combinations of input data. In view of this, the effect of local variation on global level is estimated using linear perturbation theory [11]. The propagation of variability from global modes to response is strongly non-linear. This restricts further simplification. In this study, a perturbation relating local and global modes along with a Monte-Carlo simulation is used in estimating the variability in energy influence coefficients and apparent coupling loss factors. The variability in these quantities is expected to depend on the frequency band (the number of modes in the band), the modal overlap and modal statistics [2,10].

### 3.1. Perturbation relation between local and global modal properties

The properties in each subsystem are assumed to vary randomly. In general this would require information about the statistical properties. Here certain simplifying assumption are made for convenience. First, it is assumed that the variations in the properties of one subsystem are independent of that of other subsystems. The subsystem variability could be defined in terms of component modal properties, or in terms of the elements of the subsystem mass and stiffness matrices [11]. The subsystems are then coupled using fixed interface approach to CMS. In this approach element mass and stiffness matrices can be reduced to identity and eigenvalue matrices respectively by appropriate transformation. The variability in mass and stiffness matrices is assumed to be captured by random variation of subsystem natural frequencies i.e. fixed interface eigenvalues. This approach results in computational efficiency. For simplicity, it is assumed here that the properties of the interfaces between subsystems are deterministic, and hence do not vary across the ensemble. It is also assumed that the component modal coupling matrices are deterministic. The variations from baseline eigenvalues are assumed to be small.

The variation in the  $k^{\text{th}}$  global eigenvalue [11,14], to first order, due to variation in local eigenvalue is given by

$$\delta\lambda_k = \phi_k^T \left[ \frac{\partial \mathbf{K}}{\partial \lambda_{local}} - \lambda_k \frac{\partial \mathbf{M}}{\partial \lambda_{local}} \right] \phi_k \delta\lambda_{local} \quad (43)$$

where  $\mathbf{K}$  and  $\mathbf{M}$  are global stiffness and mass matrices that are appropriately transformed to subsystem modal coordinates allowing significant reduction in dimensions of respective

matrices,  $\delta\lambda_k$  is the perturbation in  $k^{\text{th}}$  global eigenvalue,  $\lambda_{local}$  are subsystem eigenvalues and  $\phi_k$  is the  $k^{\text{th}}$  global eigenvector. With the earlier assumptions that there are no variations in the mass matrix and the coupling elements in the stiffness matrix, the variation in the  $k^{\text{th}}$  global eigenvalue due to variation in the  $j^{\text{th}}$  local eigenvalue is given by

$$\delta\lambda_k = (\phi_k)_j^2 \delta\lambda_{j,local} \quad (44)$$

The total perturbation in the  $k^{\text{th}}$  global eigenvalue is then

$$\delta\lambda_k = \sum_j (\phi_k)_j^2 \delta\lambda_{j,local} \quad (45)$$

The first order variation in the  $k^{\text{th}}$  global eigenvector [11] due to variation in the  $j^{\text{th}}$  local eigenvalue is given by

$$\delta\phi_k = \sum_j \left( \sum_{r \neq k} \frac{(\phi_k)_j (\phi_r)_j}{\lambda_k - \lambda_r} \phi_r \right) \delta\lambda_{j,local} \quad (46)$$

Using these perturbations, for an ensemble defined in terms of the statistics of the local eigenvalues, the statistics of global modes can be estimated. Knowing the statistics of these modes, a Monte-Carlo simulation can be used to estimate the propagation of perturbation to the response or the energy of the system.

#### 4. Random sampling of modes

In this section an alternative approach to randomising the structure is suggested. The aim, once again, is to randomise the structure so that the natural frequencies, mode shapes and hence energy influence coefficients are randomised. By averaging the response, robust estimates of ensemble average EICs and ACLFs can be produced.

It is proposed to randomise the system once the baseline analysis has been performed. Now, however, it is assumed that the statistics of the modes of the baseline system over a relatively wide frequency range, centred around the band of excitation, are reasonably representative of the statistics of the modes of the ensemble. The statistics required concern the natural frequencies (and their spacing) and the self- and cross-mode participation factors  $\psi_{ji}^{(r)}$  and  $\psi_{jk}^{(r)}$ .

A random sample of the modes is selected: this can be done by randomly selecting the centre frequency of the excitation band, as long as it is reasonably close to the actual centre

frequency. The closeness can be determined by expected variation in natural frequencies. Estimates of the input powers and subsystem energies are found. These are averaged to estimate the SEA ensemble average CLF matrix  $\bar{\mathbf{L}}$ , and used individually to give estimates of  $\hat{\mathbf{L}}$  from which variance, confidence limits etc can be estimated. The method requires that the modal statistics (and not the individual modal properties) vary somewhat slowly with frequency. This ensures a good “mixture” of modes, but secular effects (e.g. slow changes in modal density, group velocity, etc., with frequency) will result.

An alternative is to estimate the statistics of the baseline system with natural frequencies at and around the band centre frequency, and then to sample modes randomly using the statistics. The relevant statistics are  $\delta\omega_n$ ,  $\psi_{jj}$  and  $\psi_{jj+n}\delta\omega_n$  etc. This alternative is not considered in detail in this report.

## **5. Numerical example: Baseline structure and results for very wide frequency bandwidths**

In this section numerical examples are presented for a system comprising two coupled plates. Three different plate shapes are combined to give three systems exploring the influence of different shapes. The estimates of EICs and ACLFs are obtained for wide frequency bandwidths using modal properties found from finite element discretization and CMS approach.

The method used to obtain finite element results and then perturbations of component modes is described in [11]. The aim here is to investigate the robustness of estimated energy influence coefficients and coupling loss factors. The linear perturbation of subsystem modes is used to estimate the variability in global modes and mode shapes [11]. Then propagation of random variations in global modes and mode shapes to energy influence coefficients and coupling loss factors is evaluated using Monte-Carlo simulations. A ‘rain-on-the-roof’ excitation is used throughout. The response to ‘rain’ excitation is regarded as being equivalent to averaging the response to individual point excitations applied at all possible excitation points.

The example structures considered here are similar to those in Ref [15]. The structures comprise two coupled plates. Three shapes of plates are considered for the study; rectangular (R), distorted rectangular pentagon (D) and pentagonal (P) (Figure 1). The subsystems are discretized using the finite element package ANSYS and the mass and stiffness matrices are processed subsequently in Matlab. The subsystem modes and global modes are then obtained using the approach of fixed interface component mode synthesis (CMS). The baseline estimates of EIC and CLF are made initially using the original mass and stiffness properties. Ensemble statistics are then estimated assuming that the subsystem properties vary randomly. Instead of perturbing the system physical properties it is assumed that component level mode statistics are known and are assumed to have a normal distribution. A linear perturbation is used to estimate the variability of global modes and mode shapes. Since the perturbation from global modes to energy estimates is highly non-linear, Monte-Carlo simulations are used instead, with the response found by explicitly summing the contribution from every global mode.

Each system comprises two, straight edged plates which are edge-coupled. All edges, including the line of coupling, are simply supported. The plates are made of steel. Other properties of the plates are given in Table 1 and Figure 1 shows FE discretization.

Table 1

<i>Physical and geometric properties (SI units) for plates 1 and 2</i>			
Elastic modulus	$2 \times 10^{11}$	Length of coupled edge	0.9
Density	$8 \times 10^3$	Plate area (1, 2)	0.9, 1.26
Poisson's ratio	0.3	Modal density (1, 2)	0.0297, 0.0416
Thickness	0.01	System total modal density	0.0714

The plate areas were chosen so that the length ratio of the rectangular plates was 1.4. One plate is assumed to be excited by 'rain' of unit amplitude. The shapes of plates selected for analysis offer different amounts of irregularity. Although 9 possible combinations of two plates can be studied for their influence on the variability of estimates of coupling loss factors, the results initially are given for RR, DD and PP combinations only.

Shell elements of type 63 in ANSYS were used in discretizing the plates. General element edge length of 0.05m has been used. In the analysis only DOFs corresponding to the description of flexural motion are retained.

Figure 2 shows estimated natural frequencies for the complete system and two subsystems. For RR plates the different slopes followed by natural frequencies reflect the different modal densities of the substructures. The frequency range of 2300 Hz contains 150 global modes. About 27 modes are contained within any 400 Hz frequency band. One of the transfer mobilities with excitation on plate 1, and response location on plate 2 is shown in Figure 3. The damping loss factor of 1% was used in estimation. Below 600 Hz, the system shows strong modal behaviour. Above 1500 Hz the modal overlap is greater than 1.

For the calculation of energy influence coefficients and coupling loss factors, two centre frequencies, 500 Hz and 1500 Hz are selected. The baseline estimations are carried out with a 400 Hz frequency band. These frequency-averaged estimates are made at several damping loss factor values to assess the effect of changing modal overlap. The damping loss factor is typically varied from 0.0003 to 0.3. The modal overlap estimated is based on the centre frequency. However, in calculating cross modal power and coupling loss factors, the damping loss factor is adjusted to give the same bandwidth for any mode.

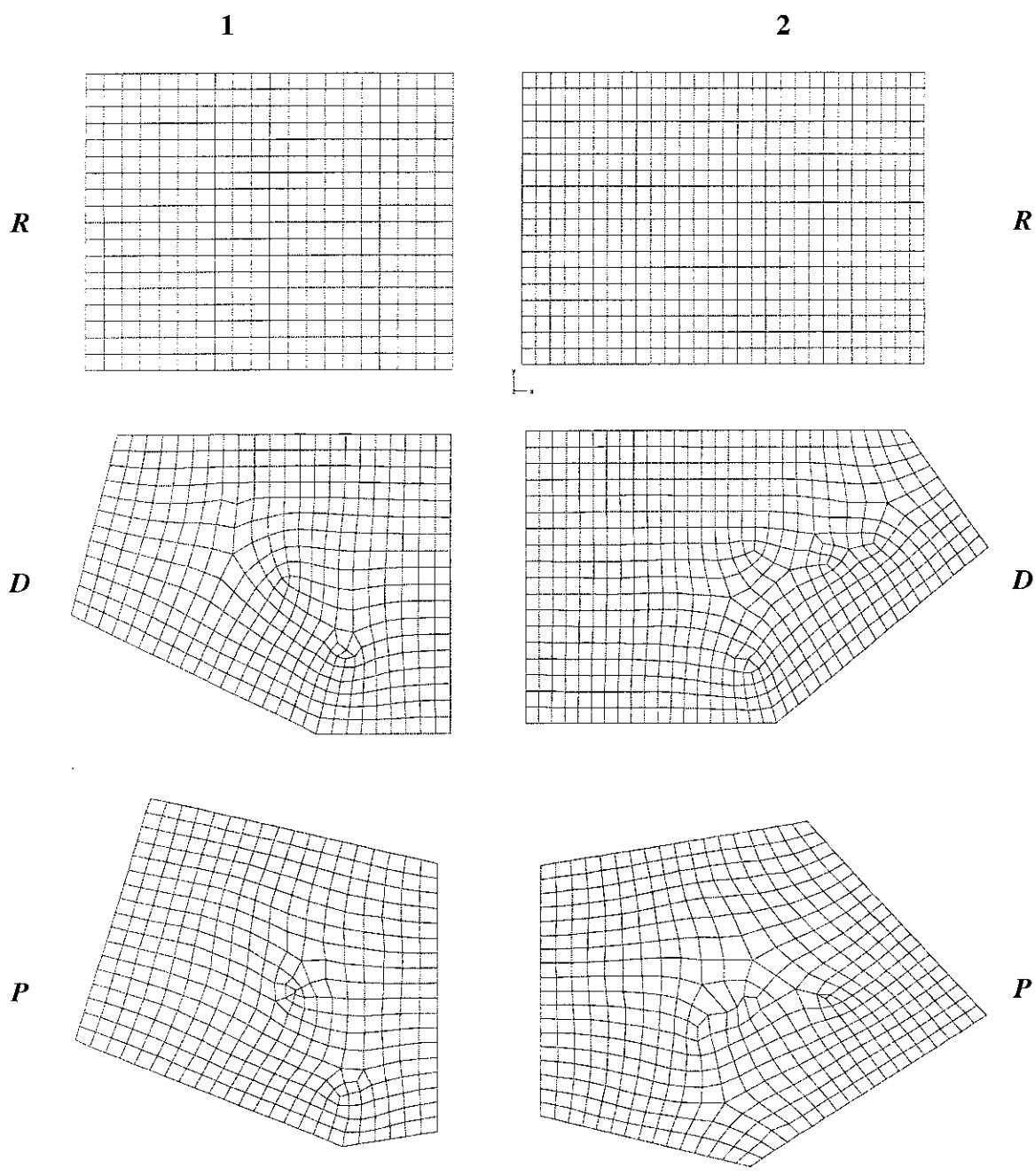


Figure 1. Finite element discretization.

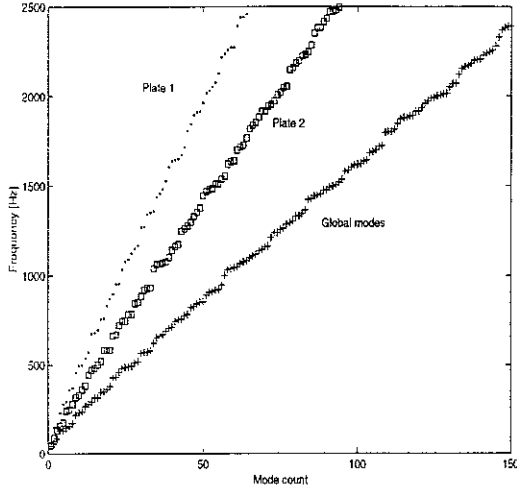


Figure 2. Natural frequencies of subsystems and total system for RR plate.

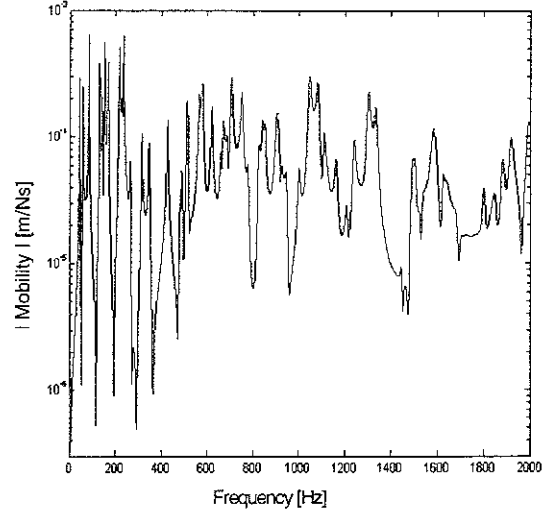


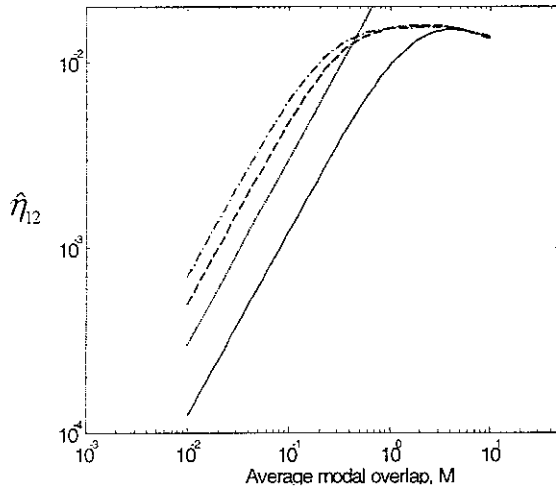
Figure 3. Example transfer mobility for RR plate.

The apparent coupling loss factors  $\hat{\eta}_{12}$  calculated for the two excitation bands centred around 500 and 1500 Hz are shown in Figure 4. Below modal overlap of about 1, the ACLFs are proportional to the damping loss factors. This is confirmed by the approximate expression for the ACLFs in this region given by

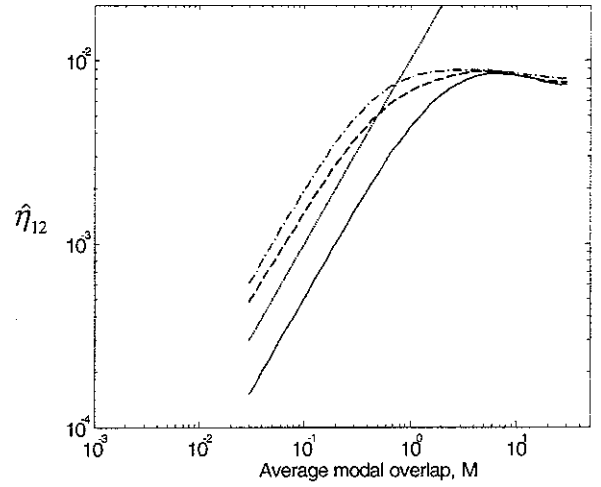
$$\hat{\eta}_{12} = \eta \frac{v_2(v_1 v_2 - \sigma_\psi^2)}{\sigma_\psi^2} \quad (47)$$

For all configurations parameters other than the damping loss factor are taken to be constant as given above. The coupling loss factor estimates converge for modal overlap larger than about 3. They converge to the value of CLF predicted by the conventional wave approximation to SEA. For PP and DD combinations of plates, the coupling loss factors converge faster compared to RR plate combination. Similar tendency is also seen for the other centre frequency (Figures 4b). The damping loss factor variation with the modal overlap is also shown in figure.

a) 500 Hz centre frequency



b) 1500 Hz centre frequency

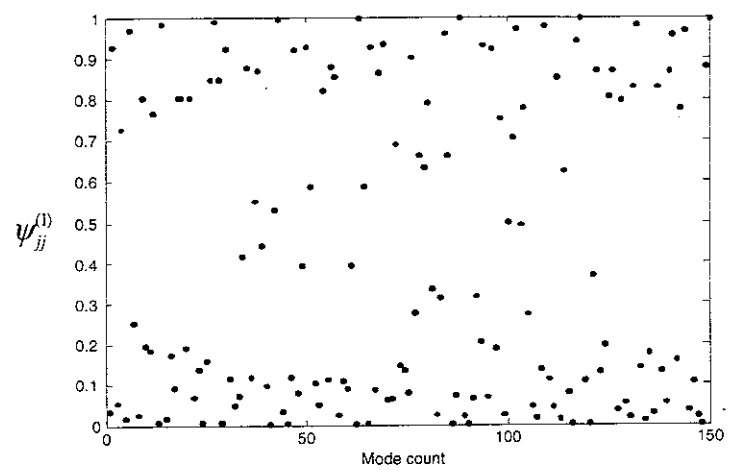


4. Variation of coupling loss factor with modal overlap: ————RR, — — — —DD, .  
 — · — · — · —PP, ······damping loss factor .

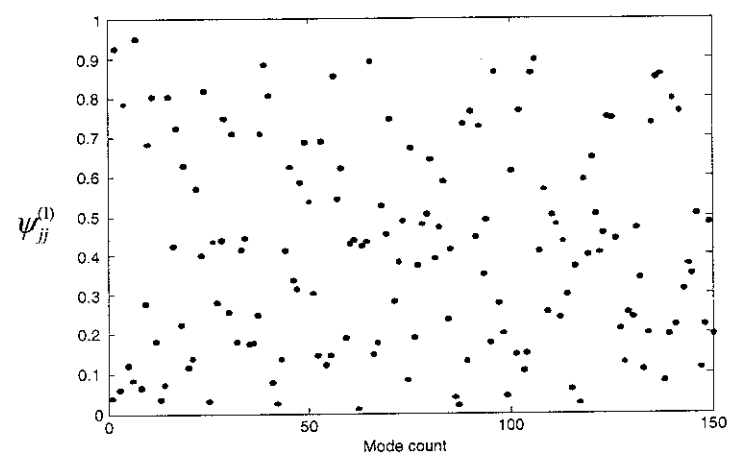
The convergence of the apparent coupling loss factors at high modal overlap is dependent on the variations seen in localization of global modes i.e. the variance  $\sigma_\psi^2$ . For low modal overlap, if the modes are more localised, then the coupling power reduces hence reducing the apparent coupling loss factor. This can also be explained using variation in the self terms of the cross modal participation factors. If the self terms are close to either 1 or 0, the modes are either contributing significantly or negligibly to the response in that subsystem. This means that the standard deviation of the participation factor tends to be large if modes are strongly localised. For a large standard deviation, referring to equation (47), the apparent coupling loss factors are smaller (provided the relative modal densities are the same). For the RR combination of plates, many of the modes are highly localised as seen in Figure 5, which shows the self terms of cross modal participation factors for the smaller plates. In contrast, the energy associated with modes tend to be spread much more evenly for the irregular PP and DD plates. This results in increased coupling power in the systems.

As the modal overlap increases, however, cross terms in cross modal power contribute significantly for any system, and hence increasing the coupling power.

a) RR



b) DD



c) PP

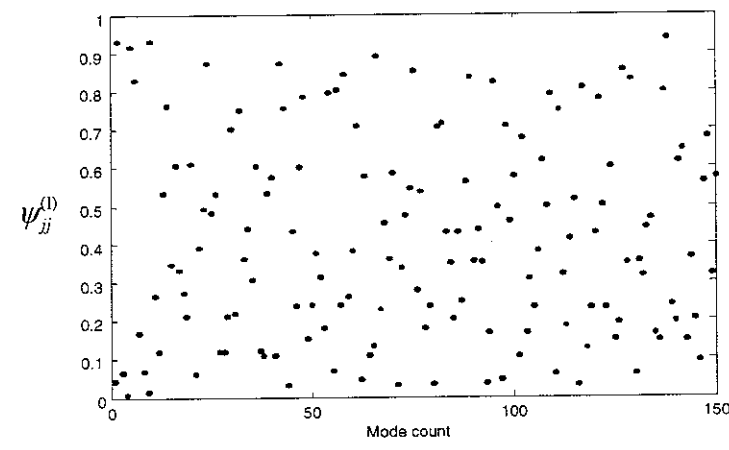


Figure 5. Self terms in modal participation factors.

### 5.1. Moderate modal overlap approximation for ACLF

In arriving at an expression for the variance of the apparent coupling loss factor at moderate modal overlap in earlier sections, it was assumed that consideration of interaction of modes with only their immediate next-neighbours would be sufficient. Figure 5 validates this assumption, where the approximate solution is seen to be accurate up to a modal overlap of around 0.7. A straight line is also shown which is taken from the expression at low modal overlap around considering only self-mode interaction. This suggests that a good approximation to the CLF can be found from the self-terms only at low modal overlap (equation (19)), the self-terms and their nearest neighbours for higher modal overlap (equation (21)) and a constant value (either from FEA at high modal overlap or the conventional SEA estimate for modal overlap greater than 1).

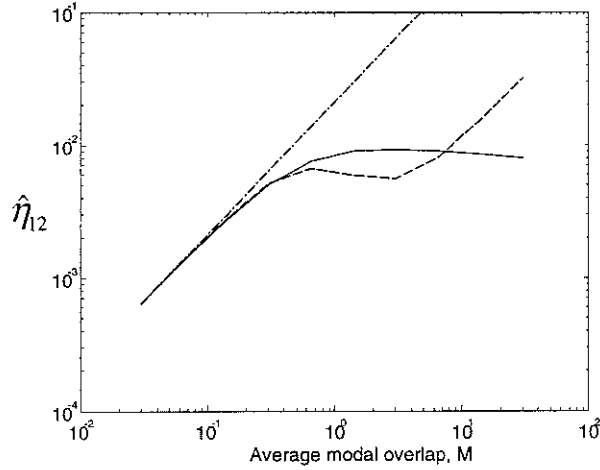
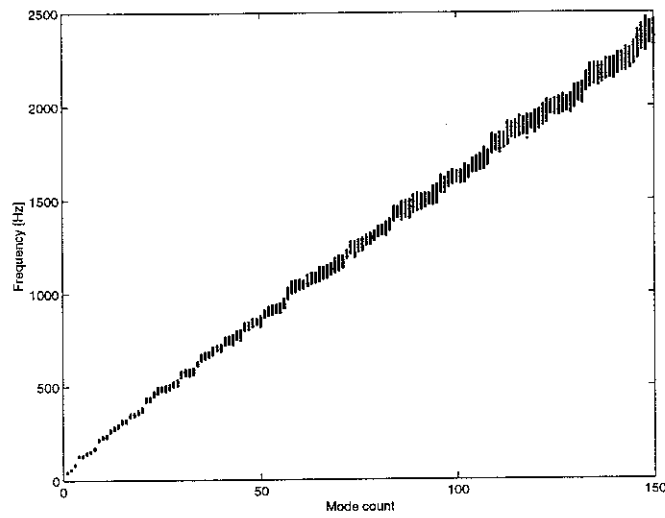


Figure 6. Approximate estimation of coupling loss factor for  $M < 0.7$ . ——— coupling loss factor, — — — moderate overlap approximation and · — · — · low modal overlap approximation.

### 5.2. ACLF statistics from the perturbational approach: numerical results

Based on the perturbation relations, Monte-Carlo simulations are used in forming ensemble estimates of energy influence coefficients and coupling loss factors. These ensemble estimates are then compared with baseline estimates to assess the effect of frequency bandwidth, modal overlap etc. For simulations, subsystem eigenvalues are assumed to have standard deviation of 2% but variations each subsystem are independent. Based on the perturbations given in equation (29), for every sample system i.e. one realization, the global modes are estimated.

Similarly, the mode shapes are evaluated using the perturbations given in equation (46). Figure 7 shows perturbed global natural frequencies for 500 realizations. As expected the absolute variability is largest for higher modes. At low frequencies the absolute variations seen are small suggesting smaller influence on frequency averaged parameters. Later, the natural frequencies are used in estimating cross modal power for any realization of the system. Before estimating cross modal participation factors, however, perturbed eigenvectors need to be mass normalized.



*Figure 7. Perturbed global natural frequencies for RR plates.*

For every realization, the energy influence coefficients and apparent coupling loss factors are estimated. The individual estimates of energy influence coefficients are then used to form the ensemble. For the SEA approach, ensemble average energy influence coefficients are used in estimating coupling loss factors. However, the average based on averaging the apparent coupling loss factors is also found so that it can be compared to the CLF estimated from ensemble average EICs.

The probability distribution of the apparent coupling loss factors for 500 realizations is calculated for every value of the modal overlap used. Figure 8 shows an example of the probability density function at very low modal overlap (0.03) for a 1500 Hz centre frequency and a 400 Hz frequency bandwidth. For such wideband, containing many modes, the variance is small. The distribution appears almost symmetrical about the arithmetic mean. In earlier studies [8-9], it was concluded that only larger modal overlaps ensure distributions that are like Gaussian. Recently, the explanation of this behaviour was discussed by Mace [10]. The

validity of application of proper-SEA at low modal overlap was confirmed in that study. Further to that, the variability in apparent coupling loss factors occurs here because of variations in the frequency band mean and variance of cross-mode participation factors for different realizations. In the low modal overlap region only the 'self' terms of the cross-mode participation factors were seen to be significant [9] (see section 2.1) and the apparent coupling loss factors are wholly dependent on the 'self' terms alone. Figure 9 shows the distribution of arithmetic mean of 'self' terms for each sample in 400 Hz frequency band at 1500 Hz central frequency. This distribution is expected to influence the distribution of the apparent coupling loss factors. In the example considered, the distribution appears slightly skewed to the right but has hardly any spread from the mean of the distribution (again, because there are so many modes in the band). This behaviour is also seen in Figure 8, even though matrix inversion is involved in estimating the apparent coupling loss factors. A close correspondence is seen in both the distributions.

Figure 10 shows confidence intervals on one of the apparent coupling loss factors for modal overlap varying from 0.03 to 30. The percentile estimates are used here to generalize the analysis which will prove helpful in later discussions where the number of modes within the frequency band are few and the probability distribution becomes non-Gaussian. The confidence interval appears to be of a similar level over the whole range of modal overlap. Also shown are the 50 percentile ACLF: the ensemble average estimate CLF, is almost identical to the 50 percentile for this case. Along with the smaller confidence band, this suggests the use of the ACLF as an alternative to the ensemble estimate when a large number of modes are within the frequency band will give very small errors. This is seen to be true whatever the value of the modal overlap. Another indicator of the equality of mean ACLF and ensemble average CLF could be that the a) arithmetic mean of distribution in Figure 9 tends to the partial modal density and b) very little variability from this mean. This would imply a confident estimate of coupling loss factors. In the next section, the influence of the number of modes and the modal overlap are investigated in assessing coupling loss factor variability.

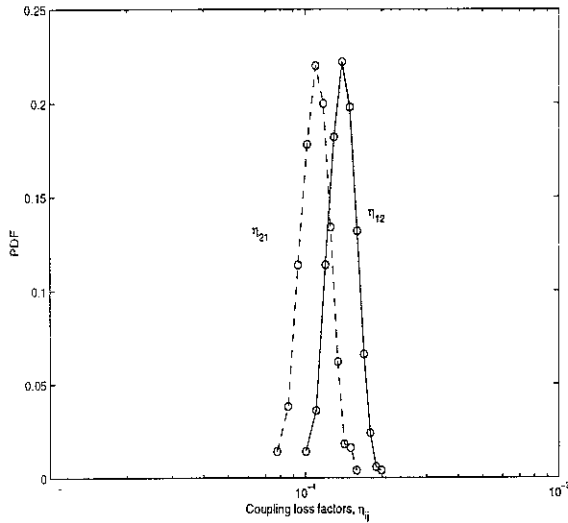


Figure 8. Probability distribution of apparent coupling loss factors at 1500 Hz, 400 Hz frequency band and 0.03 modal overlap.

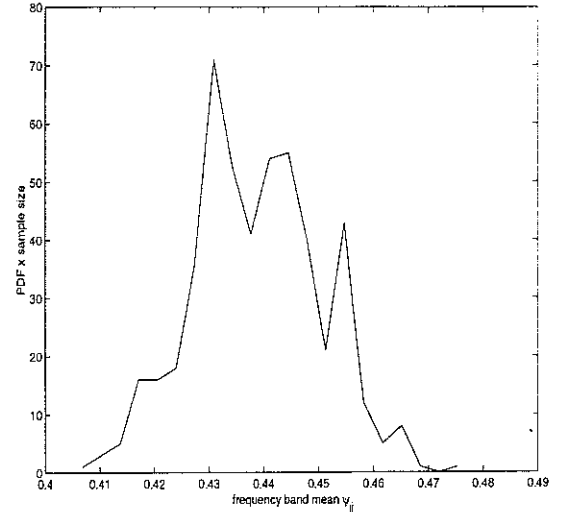


Figure 9. Probability distribution of arithmetic mean of frequency band mode participation factor at 1500 Hz, 400 Hz frequency band.

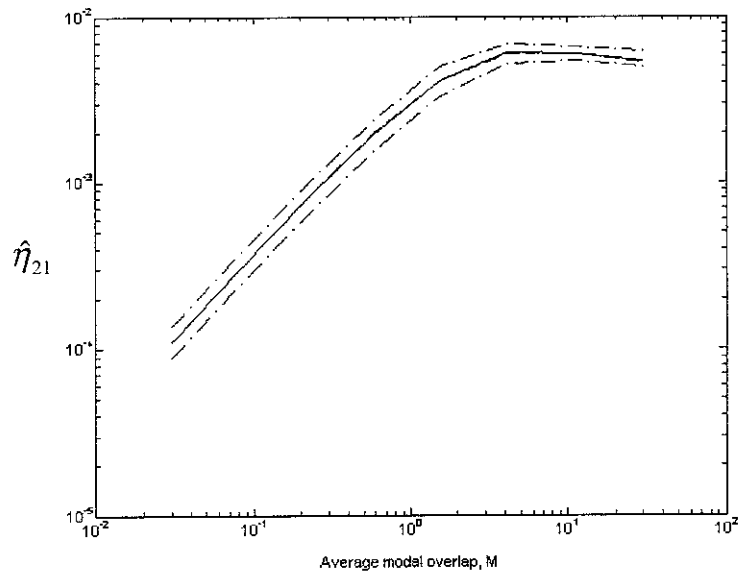


Figure 10. ACLF,  $\hat{\eta}_{21}$  at 1500 Hz, 400 Hz frequency band. ——— 50 percentile, — — — ensemble estimate CLF, — · — · — 5 and 95 percentile estimates

### 5.2.1. Effect of number of modes in band on variability

The variability of the apparent coupling loss factor in the low modal overlap region was seen by Fahy [8] not to follow any particular statistical distribution when only small number of modes was present in the frequency band. The variations might be expected to depend on the number of modes within the band. Under such conditions, the effect of certain mode lying within the band or out of it for different realizations of similar physical systems, would have a significant effect on the estimated coupling loss factors.

In this section different frequency bandwidths of 100, 50 and 30 Hz, for a centre frequency of 1500 Hz, are used to investigate the above effect. The coupling loss factors and confidence intervals for the first case are shown in Figure 11a. About 8 modes are present on average in this frequency bandwidth. A moderate increase in the confidence interval is seen in this in comparison to the 400Hz bandwidth of Figure 10. The increase is larger for smaller modal overlaps. Also, the upper and lower confidence limits are not symmetrical. The larger confidence interval for lower modal overlaps can be traced back to expressions earlier where the mode count appears in the denominator. This affects the distribution of the frequency band average of the mode participation factors. The spread here is expected to be larger than for the 400 Hz frequency bandwidth. The mean of the ACLF is also seen to differ slightly from the CLF. This indicates lesser confidence in the estimates.

Figure 11b shows results for a 50 Hz frequency bandwidth. On average, 4.8 modes are present in the frequency band. The confidence intervals are significantly larger for low modal overlaps. The average ACLF is also significantly larger than the CLF, indicating larger uncertainty. The uncertainty, as discussed earlier, is related to a larger variation of frequency band average of the mode participation factors. Similar trends are seen for a 30 Hz frequency band, shown in Figure 11c in which 3.6 modes are present on average. The confidence intervals are larger still. Again the average of ACLF deviates significantly from the CLF.

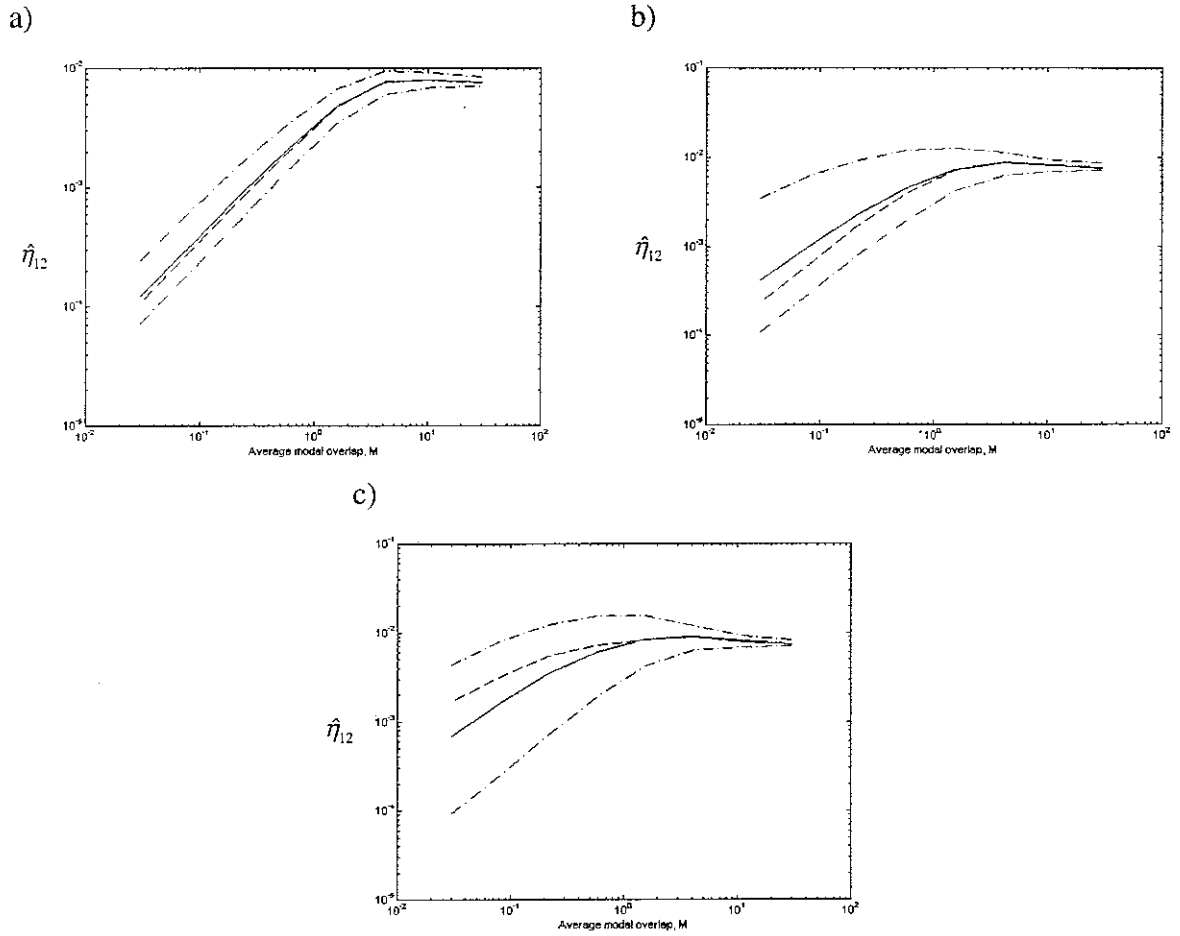


Figure 11. Apparent coupling loss factor  $\hat{\eta}_{12}$  alongwith confidence intervals for RR plates at centre frequency of 1500 Hz with frequency bandwidth - a) 100 Hz b) 50 Hz and c) 30 Hz.  
 ——— apparent coupling loss factor, — — — ensemble estimate CLF, — · — · — confidence interval.

The variation in probability density function of the ACLFs for three values of modal overlap are shown in Figure 12. As expected, a high value of modal overlap (Figure 12c) results in a more symmetric distribution of the apparent coupling loss factors and also their spread reduces. Overall, in the numerical experiments, it was seen that if more than 4 modes present in the bandwidth of excitation the estimate of ACLF is reliable at modal overlaps larger than 1. Under such circumstances, estimates with different frequency band are expected to be similar. The estimates of apparent coupling loss factor are expected to be closer to the asymptotic estimate [10]. However, at low modal overlap, the differences in estimates with differing frequency bandwidths can be very large. The probability density function is clearly non-Gaussian, with there being many, small estimated ACLFs and relatively few, very large ACLFs in the numerically generated ensemble. This can be attributed to probability

distribution of the EICs which is expected to be symmetric with only positive values. The EICs that have values closer to zero result in large ACLFs upon matrix inversion.

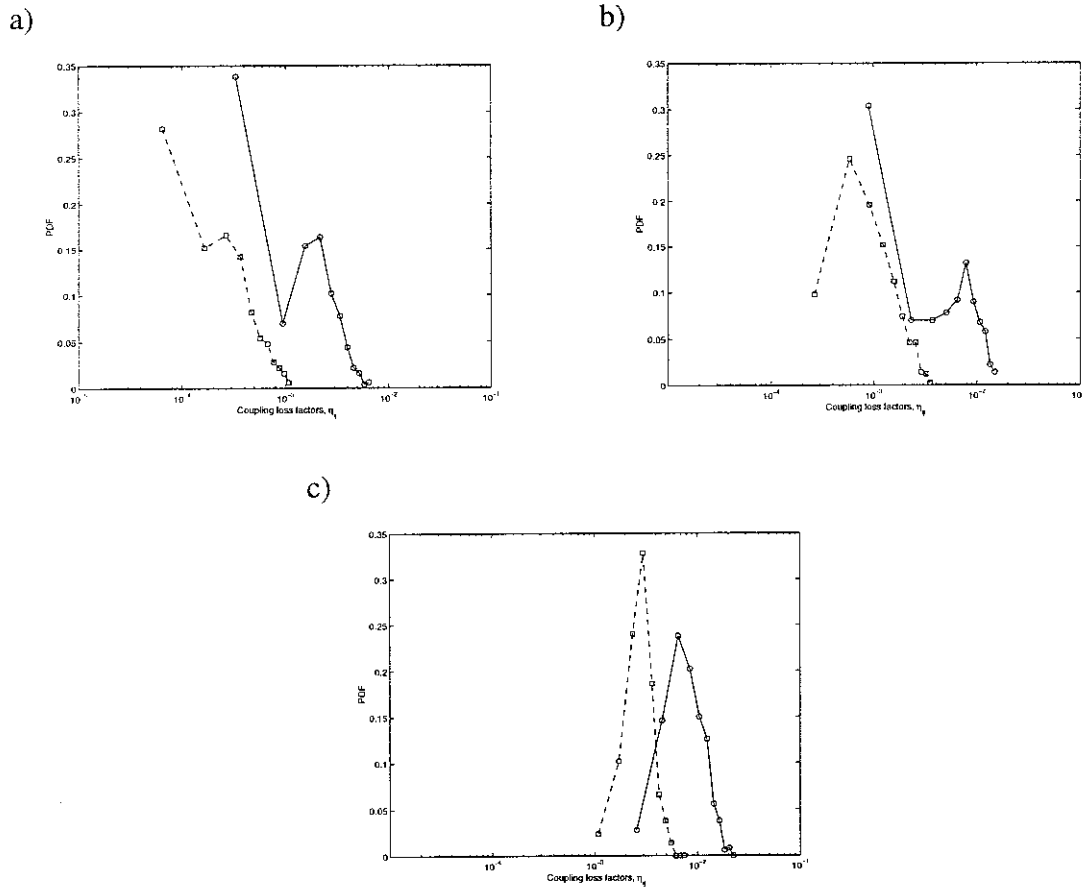


Figure 12. Apparent coupling loss factor distribution at 1500 Hz centre frequency and 30 Hz frequency band. Increasing modal overlap from a) 0.03 b) 0.16 to and c) 1.55.

————  $\hat{\eta}_{21}$  and      - - - -  $\hat{\eta}_{12}$

Another aspect of coupling loss factor variability is that, if the number of modes within the band is the same for every realization and variations occur only in mode shapes, the variability apparent in coupling loss factors is seen to be very small compared to the case where the number of modes within the band also varies. It may be sufficient to estimate variability due to eigenvalue perturbation alone.

### 5.3. CLF statistics from random sampling

Randomly sampling the centre frequency was suggested in section 4 as an alternative approach to randomising the system and to defining an ensemble. From the baseline analysis the modes of the baseline system are available. The aim, once again, is to randomise the

structure so that the natural frequencies, mode shapes and hence energy influence coefficients are randomised. By averaging the response, robust estimates of ensemble average EICs and ACLFs were produced. As an example, Figure 13a shows confidence intervals for the apparent coupling loss factor  $\hat{\eta}_{12}$  found by this approach. Note that the mean ACLF is a slightly overestimate of the CLF, the bias in the estimate arising from the skewed probability distribution of the CLF. The system used is the same as that used in the previous section. The frequency bandwidth (excitation bandwidth) is 60Hz. Here, however, the centre frequency is randomly sampled in the range from 1430 to 1560 Hz. This range can be increased to accommodate larger variations that may occur in subsystem properties. The estimates are also made using the perturbation approach for same bandwidth, results for which are shown in Figure 13b. The confidence intervals predicted by the approaches are very similar, although they should not be compared directly, being found from simulations of different random processes.

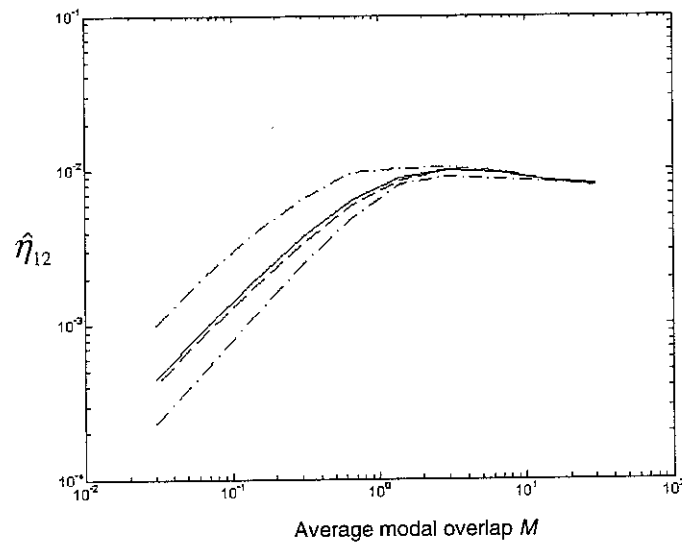


Figure 13a: Random sampling method: estimates of coupling loss factor  $\eta_{12}$  and confidence limits for RR plate at centre frequency 1500 Hz with bandwidth of 60 Hz: ——— ACLF  $\hat{\eta}_{12}$ , — — — CLF  $\eta_{12}$ , — · — · — 5% and 95% confidence intervals.

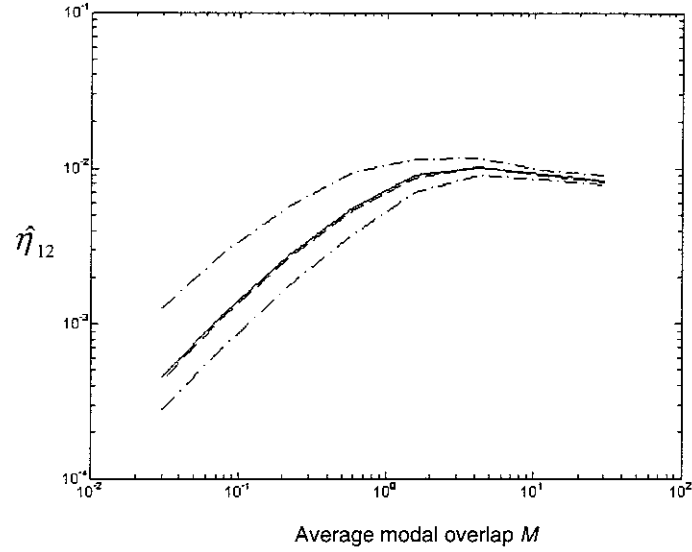


Figure 13b: Perturbational method: estimates of coupling loss factor  $\eta_{12}$  and confidence limits for RR plate at centre frequency 1500 Hz with bandwidth of 60 Hz:  
 ——— ACLF  $\hat{\eta}_{12}$ , - - - CLF  $\eta_{12}$ , - · - · - 5% and 95% confidence intervals.

## 6. Approximation with low mode count

In section 2, the expressions derived for the variance of the apparent coupling loss factors depended significantly on assumption that the number of modes in the band is large. For smaller number of modes the ratio  $\frac{N}{\overline{N}}$  might be very different from unity. Hence the expressions of section 2 will not be valid. In this section a hypothesis is proposed which approximates the variations with respect to the number of modes and the modal overlap. Before introducing the hypothesis a brief discussion is given on mode spacing statistics, which influences the number of modes present in any frequency band and influences the term  $\Gamma_{ij}$ .

### 6.1. Mode spacing

In Ref [16] and more recently [17], structural dynamic systems at high enough frequencies and with irregularity were seen to have modal statistics that follow Gaussian Orthogonal Ensemble (GOE) [18]. In the case of plates and blocks with symmetries, the modal spacing statistics was found to follow super-imposed independent GOE processes. The number of processes was seen to depend on the number of symmetries in the system. The symmetries could be in

geometry, material properties and boundary conditions. The probability density function for GOE [15] is well approximated by the Rayleigh distribution given by

$$p(x) \approx \left( \frac{\pi x}{2} \right) e^{-\frac{\pi x^2}{4}} \quad (48a)$$

where  $x$  is the spacing normalized by mean spacing. The distribution has a peak around  $x=1$  and is zero at  $x=0$  i.e. it shows level repulsion. The GOE also has statistics between next-nearest-neighbour natural frequencies etc. However, when two or more GOE processes are super-imposed the distribution does not appear to vanish at  $x=0$ . It has a finite value at this level. In structural dynamics this is the case for systems with symmetries, indicating closer spacing for some modes compared to others. If systems are symmetric, mode spacing follows Poisson distribution. The Poisson distribution is given by

$$p(x) = e^{-x} \quad (48b)$$

Figure 14a shows the natural frequency spacing distribution for the RR plates. Also shown in the figure are subsystem spacing statistics. Overall, a large number of modes are seen to be closer to each other than the mean spacing. For this case the largest concentration is seen at around 0.6 times the mean spacing. The plots shown are normalised to the mean natural frequency spacing of 14 Hz. Exponential (Poisson) distribution plot is also overlaid in figure. It can be envisaged that these spacing statistics would have some influence on the variability estimations performed in the earlier section. The chances of a mode being perturbed from within the frequency bandwidth to out of it for any realization of the system in the ensemble increases with this kind of spacing distribution. This would have significant affect on the coupling loss factor variability estimations when fewer modes are present in the frequency band. Hence, the chances of larger variability might be higher with symmetric systems due to the effect of mode spacing, however, depending on the mode shapes involved.

For plate combinations DD and PP, the mode spacing distributions are shown in Figure 14b-c. The symmetries are clearly broken compared to the case of RR plates, and most of the mode spacings are fairly close to the mean spacing. A Rayleigh distribution is also shown on the graphs. Overall, it is seen to match the distributions of the actual structures reasonably well.

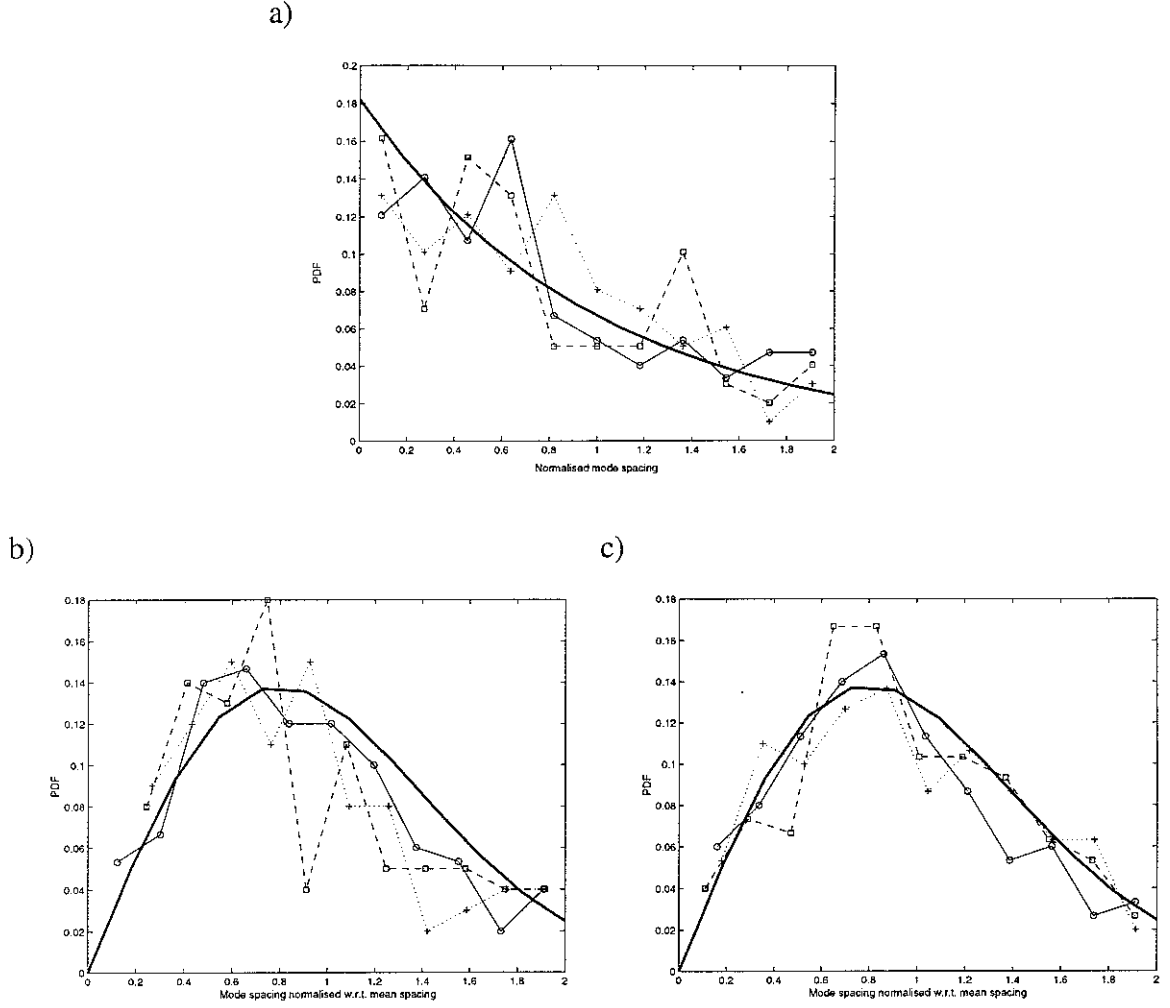


Figure 14. Mode spacing distribution. ——— system, — — — subsystem 1 (small plate) and - - - - subsystem 2 (large plate). a) RR plates  $\blacksquare \blacksquare \blacksquare \blacksquare$ . Poisson distribution b) DD plates and c) PP plates.  $\blacksquare \blacksquare \blacksquare \blacksquare$ . Rayleigh distribution.

## 6.2. Hypothesis

The confidence intervals estimated earlier for RR plates were seen to reduce with the modal overlap and increasing mode count. Expressions were derived in section 2, for situations where large number of modes were present in the bandwidth. For small number of modes in the bandwidth a modification is made here by replacing  $N$  by  $N^2$  in equation (35b) which is seen to represent variations well in this region. Therefore, the relative standard deviation variation is given by

$$\frac{\sigma}{\eta_{ij}}^{(N)} = \frac{\sigma}{\eta_{ij}}^{(N_{ref})} \frac{N_{ref}}{N} \quad (49)$$

where  $N_{ref}$  is the reference value of mode count. Figure 15 shows the variation of relative standard deviation with mode count. For both coupling loss factors, despite some discrepancies, the hypothesis seems to provide a reasonable estimate of relative standard deviation. In case of large number of modes present in the band, however, the expression derived in section 2 can be used.

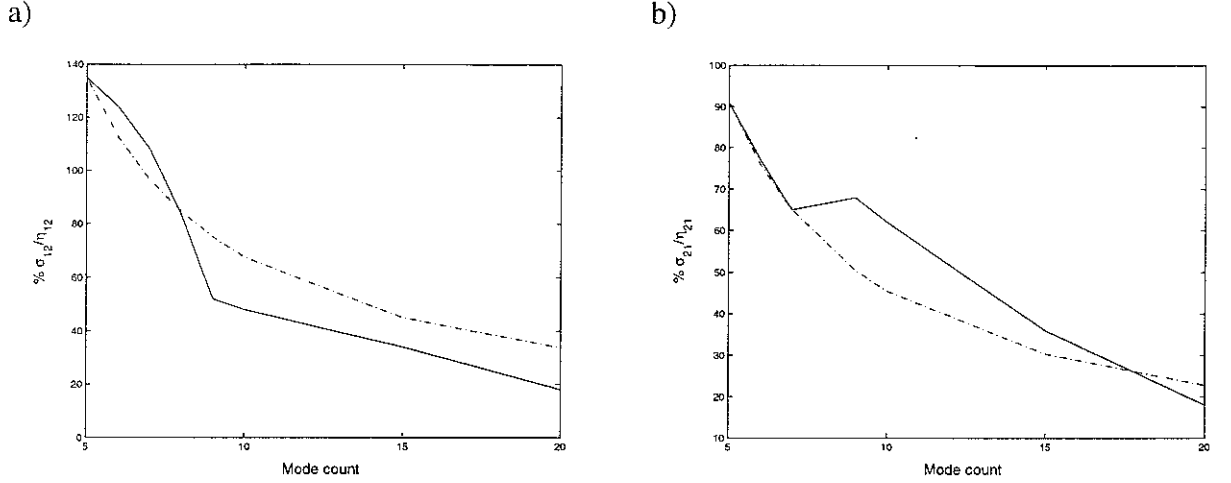


Figure 15. Influence of mode number-RR plate combination.  $\cdot \cdot \cdot \cdot \cdot$  hypothesis and  $\text{—}$  observed. a)  $\hat{\eta}_{12}$  and b)  $\hat{\eta}_{21}$ .

For low modal overlap only the influence of the self-terms in the cross-mode participation factors was found significant. It was also clear that the variations in mode shapes have negligible effect compared to whether the mode is within the frequency band or not. It might be possible to estimate the confidence interval for any system by a) establishing possible approximate relationship for the trend of the relative variance of coupling loss factor with varying modal overlap and b) estimating the relative variance of the apparent coupling loss factor at low or high modal overlap. The first step then would be to find the manner in which the confidence interval becomes smaller for increasing modal overlap. It is suggested that the confidence interval estimates are related by the approximate relationship

$$\frac{\sigma}{\eta_{ij}}(M) = \frac{\sigma}{\eta_{ij}}(M_{ref}) \frac{(1 + M_{ref})}{(1 + M)} \quad (50)$$

where  $M_{ref}$  is the reference value of the modal overlap. Figure 16 shows estimates for two bandwidths. In both cases the hypothesis provides reasonable estimates of the relative standard deviation. Some errors occur at high modal overlap for larger bandwidth. In general, estimates for values of modal overlap up to 2 can be taken as reasonable.

The combined effect of mode count and modal overlap is thus incorporated in the hypothesis,

$$\frac{\sigma}{\eta_{ij}}(M,N) = \frac{\sigma}{\eta_{ij}}(M_{ref}, N_{ref}) \frac{N_{ref}}{N} \frac{(1+M_{ref})}{(1+M)} \quad (51)$$

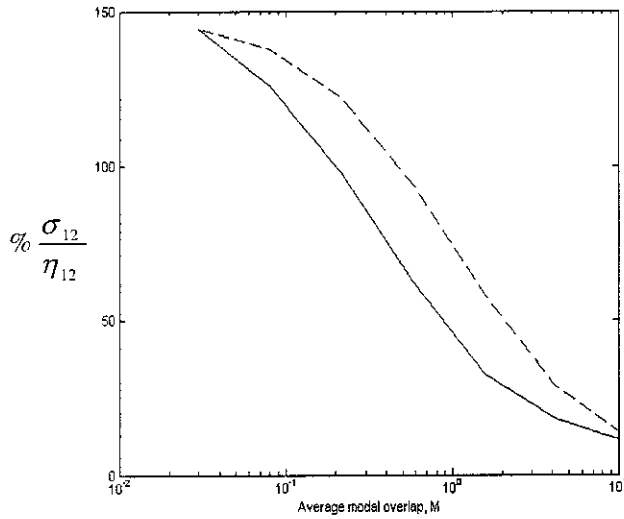
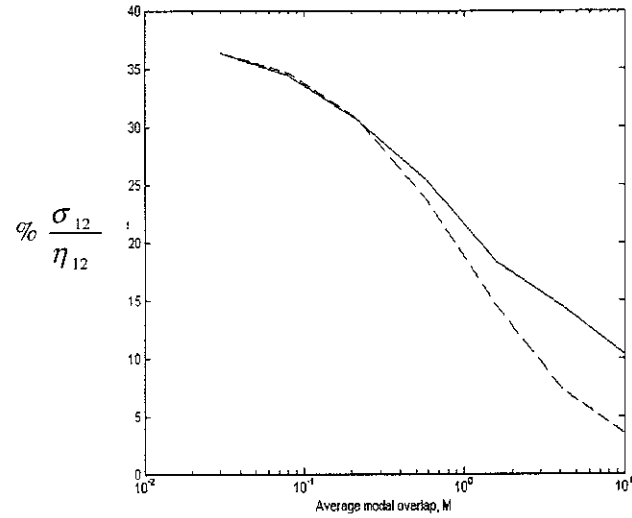


Figure 16a. RR plates - Relative standard deviation variation with modal overlap – average 6 modes in band. — perturbation based, — — hypothesis.



16b. RR plates - Relative standard deviation variation with modal overlap – average 8 modes in band. — perturbation based, — — hypothesis.

## 7. Numerical results for various shapes

In this section the effect of geometric shape of subsystems is investigated for its influence on the variability in estimates of coupling loss factors. Figure 17a shows confidence intervals on coupling loss factor for DD plates. The comparison of this with Figure 11c for RR plates shows significant reduction in the width of confidence interval at low modal overlaps. This reduction is explained by combined effect of the distribution of mode spacing and the type of mode shapes involved. Based on discussion in section 6, the mode count variance for DD plates is expected to be smaller than RR plates, indicating smaller variability for DD plates. This reduced spread in mode count ultimately results in smaller confidence intervals. The case of PP plates, shown in Figure 17b, is similar.

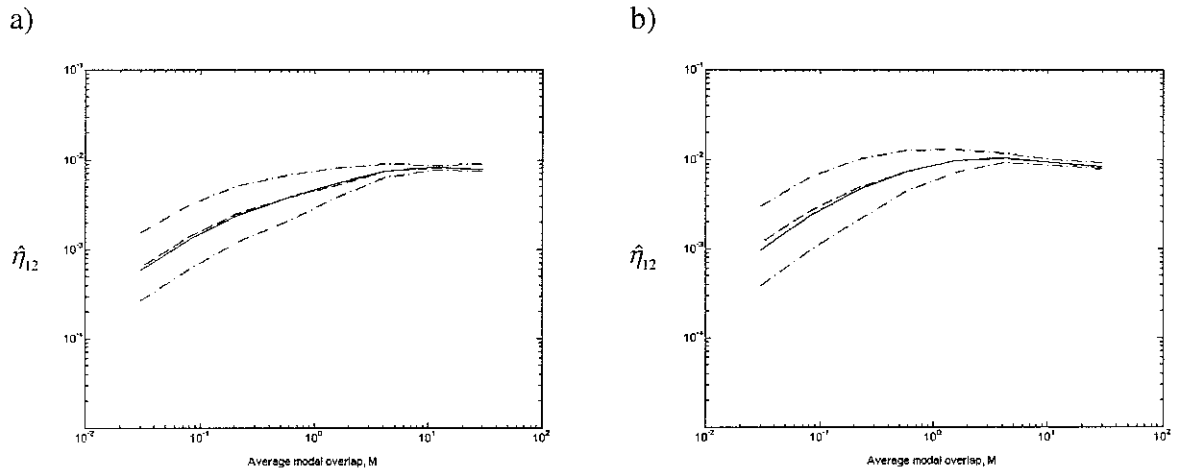


Figure 17. Apparent coupling loss factor  $\hat{\eta}_{12}$  and confidence intervals at 1500 Hz with 30 Hz frequency band. a) DD plates and b) PP plates. ——— apparent coupling loss factor, — — — ensemble estimate CLF, — · — · — confidence interval.

The hypothesis concerning the dependence of the relative standard deviation on mode count and modal overlap is also demonstrated for these shapes. Figure 18 shows the mode count dependence for DD and PP plates. Both coupling loss factors are seen to follow the trend approximated by hypothesis.

Encouraging results are also seen for modal overlap trend. This is shown in Figure 19a and b for DD and PP plates respectively. Overall, the hypothesis appears to provide a reasonable indication of the variation of the relative standard deviation.

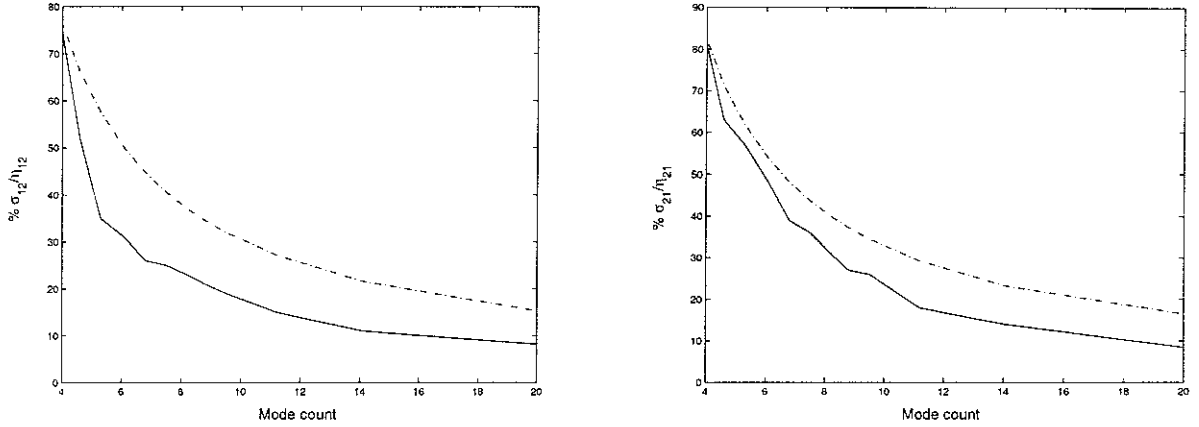


Figure 18a. Influence of mode number for DD plate combination. · — · — · — hypothesis and ——— observed.

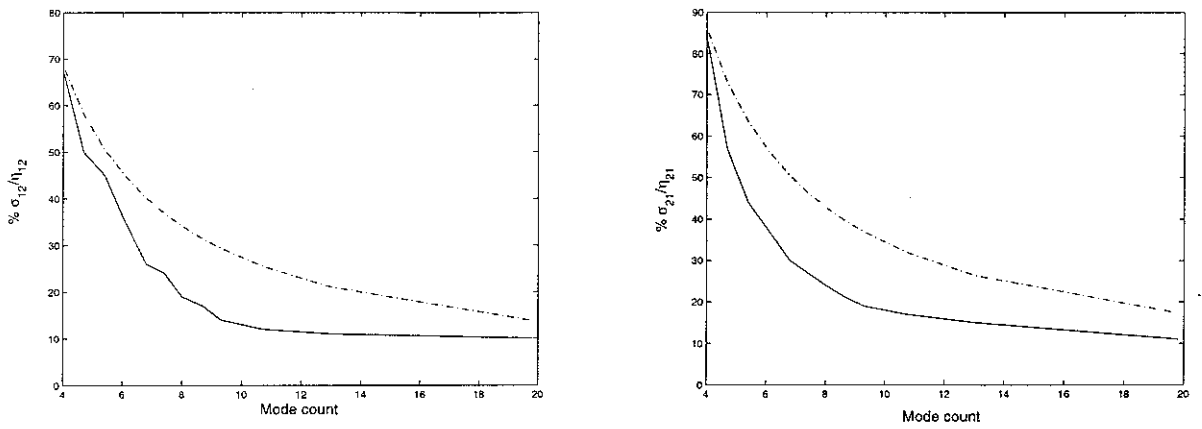


Figure 18b. Influence of mode number for PP plate combination. · — · — · — hypothesis and ——— observed.

## 8. Discussion and Conclusions

The numerical experiments have been performed to assess the robustness of estimated apparent coupling loss factors. Finite element and CMS approaches have been used in base line estimations. The LMP approach along with Monte-Carlo simulations were used in establishing ensemble response statistics. Along with robust estimation of coupling loss factors, estimates of variance, confidence limits etc can also be found in this process. Differences between the estimated CLFs (i.e. the ACLFs) and the SEA ensemble average values arise for various reasons.

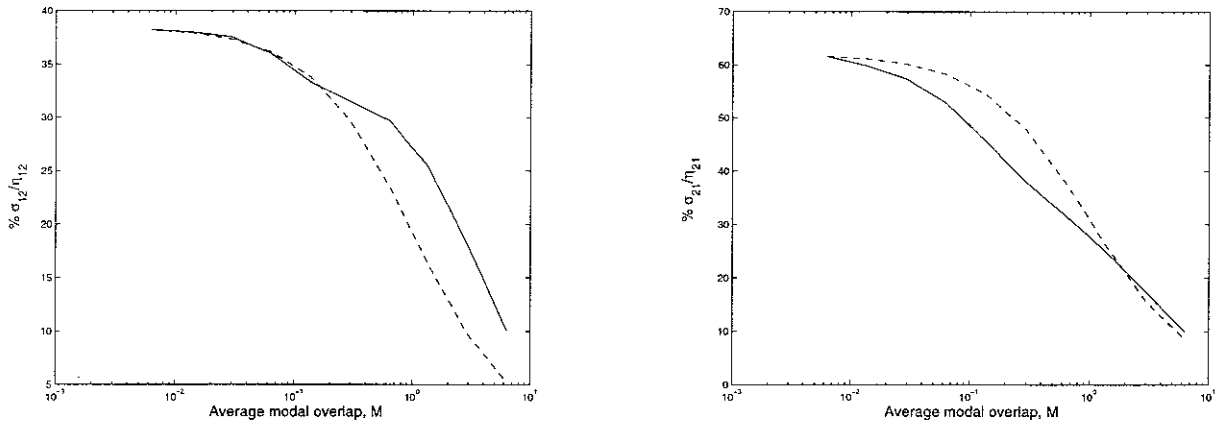


Figure 19a. DD plates - Relative standard deviation variation with modal overlap – average 6 modes bandwidth. ——— perturbation based, — — — hypothesis.

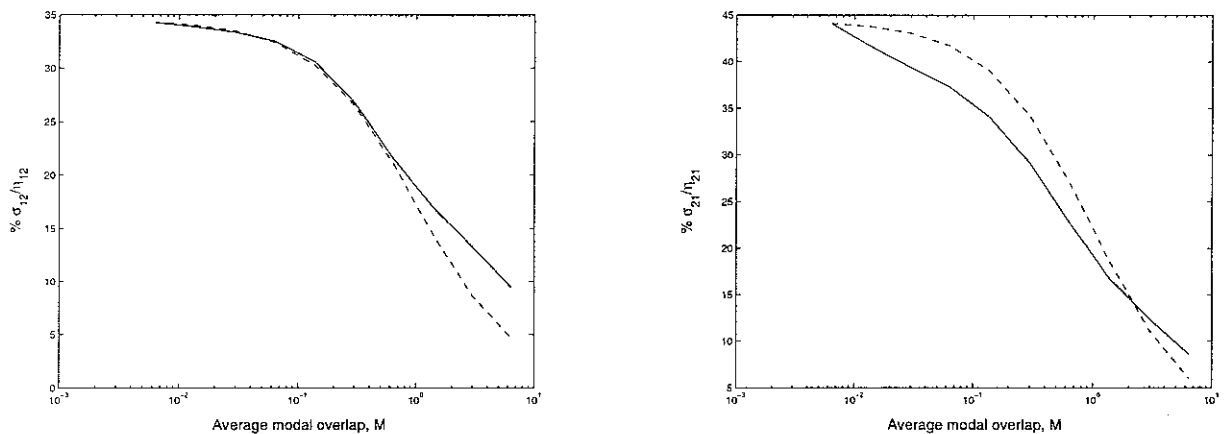


Figure 19b. PP plates - Relative standard deviation variation with modal overlap – average 6 modes bandwidth. ——— perturbation based, — — — hypothesis.

It was first noted that averaging over a finite number of excitation and response points is unnecessary, since the input powers and subsystem energies can be found exactly from the subsystem mass and stiffness matrices. These matrices must have already been determined in order that the modes of the system can be found. Then two further approaches were suggested. They both involved attempts to randomise the properties of the system being analysed, with averages being taken over the responses of various such systems. The first, the perturbational approach involved component modal descriptions of the individual subsystems. Perturbations of the subsystem modal properties can be related to perturbations in the modes of the assembled structure and hence to the energies and CLFs. The second approach assumed

that the statistics of the modal properties (natural frequencies and modes shapes) of the system analysed by FEA are a fair representation, when taken over a wide enough frequency range, of the statistics of the modes of the SEA ensemble. The modes of the system are randomly sampled to provide robust estimates of CLF, together with estimates of variance, confidence limits etc. Numerical examples were presented.

In the region of low modal overlap, the statistics of cross-mode participation factors and natural frequency spacing within the frequency band are found to be important in determining the reliability of estimated apparent coupling loss factors. When small number of modes are present within the frequency band, the larger spread of the frequency band mean of 'self' cross-mode participation factors results in the larger confidence intervals being larger. Since the irregular shapes were seen to have smaller spreads of both the frequency band mean of 'self' cross-mode participation factors and natural frequency spacing, they are seen to have smaller confidence intervals.

A hypothesis was suggested that relates the relative standard deviation to the modal overlap and mode count. The results were encouraging for values of modal overlap of up to 2. Above this value variability is typically small, in any event. This gives guideline for variations with respect to mode count and modal overlap. Provided some initial estimates are available, the qualitative assessment of influence of damping and mode counts can be carried out.

The methods are computationally very cheap. They have been developed and implemented as post-processors to the output of a conventional FE package, with the information required including the subsystem mass and stiffness matrices. The perturbational method might provide good estimates of CLFs, variance and confidence limits if there are many modes in the band or if the bandwidth is small enough and the uncertainty large enough. The random sampling approach, on the other hand, might provide good estimates if the mode statistics do not vary much with frequency. The accuracy of any estimates depends, of course, on the actual nature of variability across the ensemble of systems being analysed with the implicit assumption, in SEA, that such variability is large.

### **Acknowledgement**

The authors gratefully acknowledge the financial support provided by the Leverhulme Trust.

## 9. References

1. R.H. Lyon, R.G. DeJong, *Theory and Applications of Statistical Energy Analysis*, 2<sup>nd</sup> edition, Butterworth-Heinemann, Boston, 1995.
2. B.R. Mace, *Statistical Energy Analysis, energy flow models and System Modes*, Journal of Sound and Vibration **264**, 429-461, 2003.
3. R Langlely, *A derivation of the coupling loss factors used in statistical energy analysis*, Journal of Sound and vibration **141**, 207-219, 1990.
4. F.F. Yap, J. Woodhouse, *Investigation of damping effects on statistical energy analysis of coupled structures*, Journal of Sound and vibration **197**, 351-371, 1997.
5. E.C.N. Wester and B.R. Mace, *Statistical energy analysis of two edge-coupled rectangular plates: ensemble averages*, Journal of Sound and vibration **193**, 793-822, 1996.
6. B.R. Mace and P.J. Shorter, *Energy flow models from finite element analysis*, Journal of Sound and Vibration **233**, pp. 369-389, 2000.
7. C.R. Fredö, *SEA-like approach for the derivation of energy flow coefficients with a finite element model*, Journal of Sound and Vibration **199**, pp. 645-666, 1997.
8. F.J. Fahy, A.D. Mohammed, *A study of uncertainty in applications of SEA to coupled beam and plate systems. Part 1: computational experiments*. Journal of Sound and vibration **158**, 45-67, 1992.
9. C. Hopkins, *Statistical Energy Analysis of coupled plate systems with low modal density and low modal overlap*. Journal of Sound and vibration **251**, 193-214, 2002.
10. B.R. Mace, *Statistical energy analysis: coupling loss factors, indirect coupling and system modes*. Journal of Sound and vibration, *in print*.
11. B.R. Mace and P.J. Shorter, *A local modal/perturbational method for estimating frequency response statistics of built-up structures with uncertain parameters*, Journal of Sound and Vibration **242**, pp. 793-811, 2001.
12. J.S. Bendat and A.G. Piersol, *Random data: Analysis and measurement procedures*. John Wiley and Sons, 2000.
13. R.R. Craig, *An introduction to computer methods*. John Wiley and Sons, 1981.
14. R.L. Fox and M.P. Kapoor, *Rates of change of eigenvalues and eigenvectors*. AIAA Journal **6**(12), 2426-2429, 1968.
15. B.R. Mace and J. Rosenberg, *The SEA of two coupled plate: An investigation into the effects of subsystem irregularity*. Journal of Sound and vibration **212**, 395-415, 1998.

16. R.L. Weaver, *Spectral statistics in elastodynamics*. Journal of Acoustical Society of America, **85**, 3, 1005-1013, 1989.
17. P. Berelsen, C. Ellegaard and E. Hugues, *Distribution of eigenfrequencies for vibrating plates*. The European Physical Journal B, **15**, 87-96, 2000.
18. M.L. Mehta, *Random Matrices and Statistical Theory of Energy Levels*. Academic press, New York, 1986.